

# Joule-Thomson inversion curves of mixtures by molecular simulation in comparison to advanced equations of state: natural gas as an example

Jadran Vrabec\*    Ashish Kumar    Hans Hasse

*Institut für Technische Thermodynamik und Thermische Verfahrenstechnik,  
Universität Stuttgart, D-70550 Stuttgart, Germany*

---

## Abstract

Molecular modelling and simulation as well as four equations of state (EOS) are applied to natural gas mixtures regarding Joule-Thomson (JT) inversion. JT inversion curves are determined by molecular simulation for six different natural gas mixtures consisting of methane, nitrogen, carbon dioxide and ethane. These components are also regarded as pure fluids, leading to a total of ten studied systems. The results are compared to four advanced mixture EOS: DDMIX, SUPERTRAPP, BACKONE and the recent GERG-2004 Wide-Range Reference EOS. It is found that molecular simulation is competitive with state-of-the-art EOS in predicting JT inversion curves. The molecular based approaches (simulation and BACKONE) are superior to DDMIX and SUERTRAPP.

*Key words: Joule-Thomson inversion, natural gas, methane, ethane, nitrogen*

---

## 1 Introduction

Due to the eminent importance of natural gas, knowledge on its thermodynamic behaviour and appropriate property models are of great interest. A property often

---

\* Corresponding author, Tel.: +49-711/685-66107, Fax: +49-711/685-66140  
*Email address:* vrabec@itt.uni-stuttgart.de (Jadran Vrabec).  
*URL:* www.itt.uni-stuttgart.de (Jadran Vrabec).

needed for applications of natural gases is the adiabatic (or isenthalpic) Joule-Thomson (JT) coefficient  $\mu$ , which is defined as the derivative of the temperature  $T$  with respect to the pressure  $p$  at constant enthalpy  $h$  and constant composition  $\mathbf{x}$

$$\mu = \left( \frac{\partial T}{\partial p} \right)_{h, \mathbf{x}}, \quad (1)$$

or, using basic thermodynamics relations,

$$\mu = - \frac{1}{c_p} \left( \frac{\partial h}{\partial p} \right)_{T, \mathbf{x}}, \quad (2)$$

where  $c_p$  is the isobaric heat capacity. The JT inversion curve, connecting all state points with  $\mu=0$ , divides the pressure-temperature plane into two regions. In the lower region,  $\mu$  is positive so that an adiabatic expansion leads to a decrease in temperature. In the upper region,  $\mu$  is negative. It can be shown that the cooling effect is maximized if an expansion starts from the inversion pressure.

The experimental determination of a fluid's JT inversion coefficient demands precise measurements of volumetric and caloric properties, while the JT inversion curve extends over a broad range of temperature and pressure. Temperature and pressure reach up to a five-fold and twelve-fold of their critical values, respectively. Experimental JT inversion curve data are therefore scarce, sometimes unreliable [1], and mostly available only for pure fluids [2]. An example for mixture data is the work of Charnley et al. [3] on e.g. carbon dioxide + nitrous oxide, carbon dioxide + ethylene. A good overview over experimental data is given in [2].

For industrial applications there is a need for a proper representation and also for the prediction of JT data, as it is not feasible to measure it for all relevant and often very different blends. Some authors, e.g., Miller [4] or Gunn et al. [5], have proposed direct representations of the JT inversion curve, which are correlations in terms of reduced temperature and pressure. They provide rule-of-thumb data for simple fluids, but have little predictive power. Significantly more valuable are proper equations of state (EOS) that contain much more thermodynamic information and are valid for a broad range of state points. Thus, extensive efforts are made to use EOS for predictions of the JT inversion curve. Examples for the use of cubic EOS are modified versions of Peng-Robinson [6,7], Redlich-Kwong [6,8], Soave-Redlich-Kwong [7], Patel-Teja [6] or other cubic EOS [9] with varying parameter functions. Both type of cubic EOS and type of parameter function strongly influence the JT inversion curve, particularly in the high temperature region. A given combination might yield good results for a specific fluid, but fails for others [6,7,8,9]. Hence, it can be concluded that cubic EOS are not generally reliable for JT inversion curve predictions.

Among mixtures, natural gases are the ones that were investigated most extensively both experimentally and theoretically so that very reliable thermodynamic data and models are available. Therefore, natural gases are excellent test systems to validate thermodynamic models for mixtures.

Natural gas from the rig is a mixture of typically seventeen components (containing methane, nitrogen, carbon dioxide, ethane, propane) [10], but usually its main component is methane [11,12]. As a natural product, it has a great variability in composition and, depending on conditions in the formation process, considerable quantities of nitrogen (up to 60 mole %), carbon dioxide (up to

mole 50 %) or ethane (up to mole 20 %) are encountered [11].

For a number of pure natural gas components, reference EOS have been developed based on a vast experimental data set considering different thermodynamic properties, e.g., methane [13], nitrogen [14], carbon dioxide [15] and ethane [16]. Reference EOS have an empirical background, but they are parameterized extremely carefully, taking also available experimental JT coefficients into account. Hence, they are regarded in this work as the best available information.

For mixtures, the National Institute of Standards and Technology (NIST) [17] provided two classical phenomenological EOS, i.e. DDMIX [18,19] and SUPERTRAPP [20]. DDMIX is an implementation of the NIST extended corresponding states model for mixtures, whereas SUPERTRAPP is based on both a modified Peng-Robinson EOS and the NIST extended corresponding states model for mixtures. Both were parameterized to experimental pure substance and mixture data. Particularly SUPERTRAPP is often used in the literature as a property model for designing cooling cycles with mixed coolants, e.g. [21,22].

There are also physically based EOS that take the different molecular interactions, like dispersion or polarity, explicitly into account; an example is the BACKONE-EOS [23]. Such EOS can be parameterized for real substances with a very small experimental data set, e.g. a few vapour-liquid equilibrium data points, as they have a good predictive power. Furthermore, the GERG-2004 Wide-Range Reference EOS [24] has become available recently, which applies the concept of reference EOS to mixtures. Here too, a vast set of experimental data, both pure substance and mixture, was used for the development.

Molecular modelling and simulation offers an interesting alternative approach for predicting thermodynamic properties. Instead of describing those macroscopic properties directly, the intermolecular interactions are described. Previous work from our group [25] has demonstrated the good predictive power of molecular models for JT inversion curves for different pure fluids, but also for the mixture air which has been modelled as a ternary system containing nitrogen, oxygen and argon. The objective of the present paper is to validate the predictive power of available molecular models by comparing the results to the four advanced EOS mentioned above using different natural gas mixtures and their most important pure components regarding JT inversion.

## 2 Molecular model and simulation method

Most publications on JT inversion curves by molecular simulation are based on the spherical Lennard-Jones (LJ) model [26,27,28,29,30,31,32,33], which is appropriate only for simple molecules like methane and the noble gases. However, this simple potential model is well suited to further develop molecular simulation techniques for determining JT inversion as reliable simulation data is available for comparison. E.g., Colina et al. [34] have chosen two different routes, i.e. via compressibility [30,31] or via thermal expansivity [32], to simulate the JT inversion curve. Work on more complex fluids is still scarce, examples are Escobedo et al. [33] (nitrogen), Chacín et al. [35] (carbon dioxide), Lísal et al. [36] (R32), Kristóf et al. [37] (hydrogen sulphide), or a recent work of our group [25] dealing with fifteen different pure substances (including methane, carbon dioxide, R134a, R143a, R152a) and the mixture air. Two publications, dealing with multi-component natural gas mixtures, should be mentioned: Escobedo et al. [33]

predicted the JT inversion curve for a seven-component system, but compared it to cubic EOS data only. A favourable comparison between simulation and experiment was presented by Lagache et al. [38] regarding the JT inversion pressure of a 20-component mixture for one specified temperature.

The effective 2CLJQ pair potential was used as molecular model here to describe the intermolecular interactions in all cases. This can be done, as only the four most common components methane, nitrogen, carbon dioxide and ethane were considered, being well suited for this modelling approach. The 2CLJQ potential is composed out of two identical Lennard-Jones sites a distance  $L$  apart (2CLJ) and a point quadrupole with momentum  $Q$  placed in the geometric centre of the molecule oriented along the molecular axis

$$u_{2CLJQ}(\mathbf{r}_{ij}, \boldsymbol{\omega}_i, \boldsymbol{\omega}_j, L, Q) = u_{2CLJ}(\mathbf{r}_{ij}, \boldsymbol{\omega}_i, \boldsymbol{\omega}_j, L) + u_Q(\mathbf{r}_{ij}, \boldsymbol{\omega}_i, \boldsymbol{\omega}_j, Q), \quad (3)$$

wherein  $u_{2CLJ}$  is the contribution of the four Lennard-Jones interactions

$$u_{2CLJ}(\mathbf{r}_{ij}, \boldsymbol{\omega}_i, \boldsymbol{\omega}_j, L) = \sum_{a=1}^2 \sum_{b=1}^2 4\epsilon \left[ \left( \frac{\sigma}{r_{ab}} \right)^{12} - \left( \frac{\sigma}{r_{ab}} \right)^6 \right]. \quad (4)$$

The quadrupolar contribution  $u_Q$ , is given by [39]

$$u_Q(\mathbf{r}_{ij}, \boldsymbol{\omega}_i, \boldsymbol{\omega}_j, Q) = \frac{3}{4} \frac{Q^2}{|\mathbf{r}_{ij}|^5} f_Q(\boldsymbol{\omega}_i, \boldsymbol{\omega}_j). \quad (5)$$

Herein,  $\mathbf{r}_{ij}$  is the centre-centre distance vector of two molecules  $i$  and  $j$ ,  $r_{ab}$  is one of the four Lennard-Jones site-site distances;  $a$  counts the two sites of molecule  $i$ ,  $b$  counts those of molecule  $j$ . The vectors  $\boldsymbol{\omega}_i$  and  $\boldsymbol{\omega}_j$  represent the orientations of the two molecules  $i$  and  $j$ .  $f_Q$  is a trigonometric function depending on these molecular orientations, cf. [39]. The Lennard-Jones parameters  $\sigma$  and  $\epsilon$  represent size and energy, respectively. 2CLJQ models have the four state independent

model parameters  $\sigma$ ,  $\epsilon$ ,  $L$ , and  $Q$ , which have been adjusted to experimental vapour pressure, bubble density and critical temperature in a recent work of our group [40]. All pure substance parameters are given in Table 1. The spherical non-polar LJ model for methane is a limiting case of 2CLJQ models, where  $L = 0$  and  $Q = 0$ .

To perform simulations of mixtures, a molecular mixture model is needed. On the basis of pairwise additive pure fluid models, molecular modelling of mixtures reduces to modelling interactions between unlike molecules. Here, the modified Lorentz-Berthelot combining rule with one adjustable binary interaction parameter  $\xi$  was used for each unlike Lennard-Jones interaction

$$\sigma_{ij} = \frac{\sigma_i + \sigma_j}{2}, \quad (6)$$

$$\epsilon_{ij} = \xi \cdot \sqrt{\epsilon_i \cdot \epsilon_j}. \quad (7)$$

The state independent parameter  $\xi$  was adjusted to one experimental vapour pressure of each binary mixture in prior work of our group [41,42,43]. Table 2 reports the six binary parameters of the quaternary natural gas mixture model. The unlike quadrupolar interactions are treated in a physically straightforward way, following the laws of electrostatics without any binary parameters. It should be pointed out, that exclusively experimental VLE data were used in the parameterization of the molecular mixture model, but no caloric data.

For the calculation of JT inversion curves on the basis of a given model by molecular simulation, several methods have been proposed in the literature [30,31,32,44]. Here, as in prior work [25], an intuitive and straightforward method was used. To calculate one JT inversion pressure  $p$  for a given temperature  $T$ , a series of

simulations, generally from 5 to 10, were made around the expected result, covering typically a rather large pressure range of 20 MPa. In these simulations, the enthalpy  $h$  and its partial derivative with respect to pressure  $(\partial h/\partial p)_{T,\mathbf{x}}$  were calculated. Both data sets were fitted simultaneously by a second order polynomial vs. pressure at that particular temperature. The inversion pressure corresponds simply to the minimum value of enthalpy, i.e. the minimum of that quadratic fit.

Molecular dynamics simulations were performed in the isobaric-isothermal ( $NpT$ ) ensemble, using Andersen's barostat [45] and isokinetic velocity scaling [46] for thermostating. After 6 000 equilibration time steps, the residual enthalpy [47]

$$h^{res} = \frac{1}{N} \cdot \left\{ \left\langle \sum_{i=1}^N \sum_{j>i}^N u_{2CLJQ}(\mathbf{r}_{ij}, \boldsymbol{\omega}_i, \boldsymbol{\omega}_j, L, Q) \right\rangle + p \langle V \rangle \right\} - k_B T, \quad (8)$$

was averaged over 200 000 time steps, where the first term indicates the simulation average over the intermolecular potential energy and  $\langle V \rangle$  is the average of the extensive volume. The partial derivative was obtained by a fluctuation expression [48]

$$\left( \frac{\partial h^{res}}{\partial p} \right)_{T,\mathbf{x}} = \frac{1}{N} \cdot \left\{ \frac{1}{k_B T} \cdot [\langle V \rangle \langle H^{res} \rangle - \langle V H^{res} \rangle] + \langle V \rangle \right\}, \quad (9)$$

where  $H^{res}$  is the extensive residual enthalpy. The ideal part of the enthalpy is not relevant, as it is not pressure dependent.

Depending on the density of the state point, the membrane mass parameter  $M$  of Andersen's barostat [45] was chosen from  $10^{-20}$  to  $10^{-15}$  kg/m<sup>4</sup>. The intermolecular interactions were evaluated explicitly up to a cut-off radius of  $r_c = 5\sigma$  and standard long range corrections were used for the Lennard-Jones interaction,



employing angle averaging as proposed by Lustig [49]. Long-range corrections for the quadrupolar interaction are not needed since they disappear. A total number of  $N = 1372$  molecules were initially placed in a fcc lattice configuration into a cubic simulation box, where the density of the system was chosen close to that expected from an EOS, if available, otherwise estimates were used.

### 3 Results

JT inversion curves are compared for six different systematically chosen gas mixtures consisting of the four main natural gas components methane, nitrogen, carbon dioxide and ethane. Firstly, the three methane containing binary systems that can be formed from these four components were studied at equimolar composition, where the highest effect of mixing can be expected. Following this, secondly, all three ternary systems containing methane were studied, again at equimolar composition, i.e. with a mole fraction  $x_i = 1/3$  throughout. Finally, also the four pure fluids were investigated.

Simulation results for pure methane and carbon dioxide were taken from prior work [25], but for nitrogen and ethane as well as for all mixtures new simulation results are presented. Tables 3 and 4 compile the full simulation data set. The statistical uncertainties of this data are estimated to be in the order of 1 MPa. This translates into a relative error of around 2 % for medium temperatures, but the relative errors are considerably larger at extremely low and high temperatures, where the inversion pressure approaches zero.

For all systems the results for the JT inversion curves from molecular simulation are compared to the four mixture EOS, i.e. DDMIX [18,19], SUPERTRAPP

[20], BACKONE-EOS [23] and GERG-2004 [24]. The pure substance results are additionally compared to reference EOS using the program package REFPROP [50]. All results are presented in pressure-temperature diagrams as well as in deviation plots.

### *3.1 Pure components*

Figures 1 and 2 present the JT inversion curves of the pure fluids, which were grouped to achieve a good visibility. In these Figures, it can be seen that the results from the different methods qualitatively agree. Especially in the low temperature region of the JT inversion curves, they are often undistinguishable in these absolute plots. Significant deviations, however, occur for higher temperatures. For a more detailed discussion, the deviation plots in Figure 3 are more suited, where the baselines represent GERG-2004. It should be pointed out that in Figure 3 additionally the pure substance reference EOS [13,14,15,16] results are shown. GERG-2004 agrees with the reference EOS within less than about 3 % throughout, except for methane at high temperatures. DDMIX and BACKONE agree roughly equally well to GERG-2004 as well as the simulation data, often with the same trends. Generally, these results lie within a band of about 5 %, larger deviations are found particularly at high temperatures. BACKONE yields mostly higher results for high temperatures than GERG-2004, whereas DDMIX tends to yield lower values. Significantly worse is SUPERTRAPP which yields negative deviations of more than 10 % in large parts of the high temperature range of methane and nitrogen.

### 3.2 Mixtures

Figures 4 to 6 present the JT inversion curves for the six equimolar binary and ternary mixtures, which are again grouped to achieve good visibility. As for the pure fluids, the qualitative agreement between the different studied models is observed throughout. The agreement between all models is almost always excellent for low temperatures, but significant deviations are found in the high temperature region. Compared to the pure substances the spread between the different models is larger. Also here, the results can better be resolved in deviation plots, where the baselines were again chosen to represent GERG-2004 data. Figure 7 shows the binary and Figure 8 the ternary cases. Simulation data and GERG-2004 agree also for mixtures usually within 5 %, larger relative deviations are found for very high temperatures. BACKONE shows a comparable performance. It yields systematically higher values at strongly elevated temperatures and a better agreement with GERG-2004 than DDMIX and SUPERTRAPP. These two EOS show poorer results throughout, which are always too low by more than 10 % at high temperatures. SUPERTRAPP yields the largest deviations in all cases.

GERG-2004 was taken as a reference here as the broadest possible experimental data set was taken for its parameterization. This is confirmed by the fact that GERG-2004 data lies almost always in between the remaining results. Comparing it to the reference EOS for pure fluids, which were individually fitted including JT inversion data, an uncertainty of only about 3 % has to be assumed, except for methane at high temperatures.

## 4 Conclusion

In this work, results from molecular modelling and simulation were compared to four advanced mixture EOS regarding JT inversion curves of natural gas mixtures. With a focus on the four most important components methane, nitrogen, carbon dioxide and ethane, six different equimolar binary and ternary mixtures were selected systematically. As a reference and for completeness, the four components were also regarded as pure fluids. The comparison shows that molecular modelling and simulation is competitive with the most state-of-the-art EOS in predicting JT inversion curves. This approach has a similar performance as BACKONE, which is based on molecular simulation data itself. DDMIX and particularly SUPERTRAPP are less reliable.

It can be stated that for other mixtures, where no such elaborate EOS are available, that molecular modelling and simulation is the method of choice to predict JT inversion.

## 5 Acknowledgment

We gratefully acknowledge financial support by Deutsche Forschungsgemeinschaft, Schwerpunktprogramm 1155.

## List of symbols

$a$	interaction site index
$b$	interaction site index
$c_p$	molar isobaric heat capacity
$f_Q$	short notation for a trigonometric function
$h$	molar enthalpy
$H$	extensive enthalpy
$k_B$	Boltzmann constant
$L$	molecular elongation
$N$	number of molecules
$p$	pressure
$Q$	molecular quadrupole momentum
$r_{ab}$	site-site distance
$r_c$	center-center cut-off radius
$T$	temperature
$u$	pair potential
$V$	extensive volume
$x$	mole fraction
$\epsilon$	Lennard-Jones energy parameter
$\mu$	Joule-Thomson coefficient
$\xi$	binary interaction parameter
$\sigma$	Lennard-Jones size parameter

## Vector properties

$\mathbf{r}$	distance vector
$\mathbf{x}$	mole fraction vector
$\boldsymbol{\omega}$	orientation vector

## Subscript

$a$	interaction site index
$b$	interaction site index
$i$	molecule index
$i$	component index
$j$	molecule index
$j$	component index
Q	point quadrupole
2CLJ	two-center Lennard-Jones
2CLJQ	two-center Lennard-Jones plus point quadrupole

## Superscript

$res$	residual property
-------	-------------------

## References

- [1] M.J. Hiza, A.J. Kidnay, R.C. Miller, *Equilibrium Properties of Fluid Mixtures*, New York, IFI/Plenum, 1975.
- [2] R.H. Perry, D.W. Green (Eds.), *Perry's Chemical Engineers' Handbook*, 7th Ed., New York, McGraw-Hill, 1997.
- [3] A. Charnley, J.S. Rowlinson, J.R. Sutton, J.R. Townley, *Proc. Royal Soc. London A* 230 (1955) 354-358.
- [4] D.G. Miller, *Ind. Eng. Chem. Fundam.* 9 (1970) 585-589.
- [5] R.D. Gunn, P.L. Chueh, J.M. Prausnitz, *Cryogenics* 6 (1966) 324-329.
- [6] N.S. Matin, B. Haghighi, *Fluid Phase Equilib.* 175 (2000) 273-284.
- [7] B. Haghighi, M.R. Laee, N.S. Matin, *Cryogenics* 43 (2003) 393-398.
- [8] K. Juris, L.A. Wenzel, *AIChE J.* 18 (1972) 684-688.
- [9] B. Haghighi, M.R. Laee, M.R. Husseindokht, N.S. Matin, *J. Ind. Eng. Chem.* 10 (2004) 316-320.
- [10] D.F. Bergman, M.R. Tek, D.L. Katz, *Retrograde condensation in natural gas pipelines*, Am. Gas Assoc., Pipeline Res Committee L22277, Project PR 26-29, 1975.
- [11] Technical Note 412, United States Department of the Interior, Bureau of Land Management, *Analyses of Natural Gases*, 1998-2001.  
<http://www.blm.gov/nstc/library/pdf/TN412.pdf>.
- [12] D. Ginter, C. Simchick, J. Schlakker, *Durability of Catalytic Combustion Systems. APPENDIX VI: Variability in Natural Gas Fuel Composition and Its Effects on the Performance of Catalytic Combustion Systems*, California Energy Commission, 2001.
- [13] U. Setzmann, W. Wagner, *J. Phys. Chem. Ref. Data* 20 (1991) 1061-1155.
- [14] R. Span, E.W. Lemmon, R.T. Jacobsen, W. Wagner, A. Yokozeki, *J. Phys. Chem. Ref. Data* 29 (2000) 1361-1433.
- [15] R. Span, W. Wagner, *J. Phys. Chem. Ref. Data* 25 (1996) 1509-1596.
- [16] D.G. Friend, H. Ingham, J.F. Ely, *J. Phys. Chem. Ref. Data* 20 (1991) 275-347.
- [17] <http://www.nist.gov/>.
- [18] J.F. Ely, J.W. Magee, W.M. Haynes, *NBS standard reference database 14, DDMIX, Version 9,06*, NIST, Boulder, Colorado, 1989.
- [19] J.F. Ely, *Adv. Cryog. Eng.* 35 (1990) 1511-1520.

- [20] E.F. James, M.I. Huber, NIST Thermodynamic Properties of Hydrocarbon Mixtures Database (SUPERTRAPP). US Department of Commerce, National Institute of Standards and Technology, 1992.
- [21] B.-Z. Maytal, G.F. Nellis S.A. Klein, J.M. Pfothenhauer, *Cryogenics* 46 (2006) 55-67.
- [22] H. Huang, L.J. Spadaccini, D.R. Sobel, *J. Eng. Gas Turbines Power* 126 (2004) 284-293.
- [23] M. Wendland, B. Saleh, J. Fischer, *Energy and Fuels* 18 (2004) 938-951.
- [24] O. Kunz, R. Klimeck, W. Wagner, M. Jaeschke, The GERG-2004 Wide-Range Reference Equation of State for Natural Gases and Other Mixtures. To be published as GERG Technical Monograph. *Fortschr.-Ber. VDI*, VDI-Verlag, Düsseldorf, 2007.
- [25] J. Vrabec, G.K. Kedia, H. Hasse, *Cryogenics* 45 (2005) 253-258.
- [26] D. Bessières, S.L. Randzio, M.M. Piñeiro, T. Lafitte, J.-L. Daridon, *J. Phys. Chem. B* 110 (2006) 5659-5664.
- [27] D.M. Heyes, C.T. Llaguno, *Chem. Phys.* 168 (1992) 61-68.
- [28] C.M. Colina, E.A. Muller, *Int. J. Thermophys.* 20 (1999) 229-235.
- [29] L.I. Kioupis, G. Arya, E.J. Maginn, *Fluid Phase Equilib.* 200 (2002) 93-110.
- [30] C.M. Colina, E.A. Müller, *Int. J. Thermophys.* 20 (1999) 229-235.
- [31] C.M. Colina, E.A. Müller, *Mol. Sim.* 19 (1997) 237-246.
- [32] M. Lagache, P. Ungerer, A. Boutin, A.H. Fuchs, *Phys. Chem. Chem. Phys.* 3 (2001) 4333-4339.
- [33] F.A. Escobedo, Z. Chen, *Mol. Sim.* 26 (2001) 395-416.
- [34] C.M. Colina, M. Lísal, F.R. Siperstein, K.E. Gubbins, *Fluid Phase Equilib.* 202 (2002) 253-262.
- [35] A. Chacín, J.M. Vázquez, E.A. Muller, *Fluid Phase Equilib.* 165 (1999) 147-155.
- [36] M. Lísal, W.R. Smith, K. Aim, *Mol. Phys.* 101 (2003) 2875-2884.
- [37] T. Kristóf, G. Rutkai, L. Merényi, J. Liszi, *Mol. Phys.* 103 (2005) 537-545.
- [38] M.H. Lagache, P. Ungerer, A. Boutin, *Fluid Phase Equilib.* 220 (2004) 211-223.
- [39] C.G. Gray, K.E. Gubbins, *Theory of molecular fluids. Fundamentals*, Oxford, Clarendon Press, 1984.
- [40] J. Vrabec, J. Stoll, H. Hasse, *J. Phys. Chem. B* 105 (2003) 12126-12133.
- [41] J. Stoll, J. Vrabec, H. Hasse, *AIChE J.* 49 (2003) 2187-2198.



- [42] J. Vrabec, J. Stoll, H. Hasse, *Mol. Sim.* 31 (2005) 215-221.
- [43] Y.-L. Huang, Systematic investigation of vapor-liquid equilibria of binary mixtures on the basis of polar two-center Lennard-Jones models, MSc thesis, University of Stuttgart, 2005.
- [44] L.I. Kioupis, E.J. Maginn, *Fluid Phase Equilib.* 200 (2002) 75-92.
- [45] H.C. Andersen, *J. Chem. Phys.* 72 (1980) 2384-2393.
- [46] M.P. Allen, D.J. Tildesley, *Computer Simulation of Liquids*, Oxford, Clarendon Press, 1987.
- [47] D.W. Heermann, *Computer Simulation Methods in Theoretical Physics*. Springer-Verlag, Berlin 1986.
- [48] T.L. Hill, *Statistical Mechanics*, McGraw-Hill Book Company, New York, 1956.
- [49] R. Lustig, *Molec. Phys.* 65 (1988) 175-179.
- [50] REFPROP, NIST Standard Reference Database 23, Version 7.0:2002.

Table 1  
Parameters of pure fluid molecular models, taken from [40].

Fluid	$\sigma/\text{\AA}$	$(\epsilon/k_B)/\text{K}$	$L/\text{\AA}$	$Q/\text{D}\text{\AA}$
methane	3.7281	148.55	-	-
nitrogen	3.3211	34.897	1.0464	1.4397
carbon dioxide	2.9847	133.22	2.4176	3.7938
ethane	3.4896	136.99	2.3762	0.8277

Table 2  
Binary interaction parameters, taken from [41,42,43].

Mixture	$\xi$
methane + carbon dioxide	0.997
methane + ethane	0.958
nitrogen + methane	0.974
nitrogen + carbon dioxide	0.962
nitrogen + ethane	0.954
carbon dioxide + ethane	1.041

Table 3

Molecular simulation results for JT inversion of the pure components. Data for methane and carbon dioxide was taken from [25], the remainder is from this work.

$T / \text{K}$	$p / \text{MPa}$	$T / \text{K}$	$p / \text{MPa}$	$T / \text{K}$	$p / \text{MPa}$	$T / \text{K}$	$p / \text{MPa}$
methane		nitrogen		carbon dioxide		ethane	
178.26	15.83	100	1.81	300	29.05	250	2.83
222.83	28.43	125	12.31	350	58.80	275	12.50
267.39	41.22	150	24.68	400	76.09	300	21.58
311.96	47.53	175	31.13	450	82.32	325	29.42
356.52	50.83	200	35.78	500	87.16	350	34.94
401.09	51.73	250	39.54	550	90.27	375	40.45
445.65	51.44	300	38.88	600	91.31	425	48.80
490.22	50.58	350	36.72	650	90.62	475	53.93
534.78	48.73	400	31.55	700	87.16	500	57.38
579.35	45.68	450	24.62	750	80.94	525	58.28
623.91	42.81	500	17.37	800	76.09	600	60.14
668.48	39.56	550	8.48	850	69.18	675	60.82
713.04	33.62			900	60.87	750	56.97
757.61	27.73			950	53.96	825	54.34
802.17	22.68			1000	45.66	900	48.37
846.74	15.27			1050	37.35	975	42.13
891.30	10.68			1100	28.36	1000	38.86
935.87	6.32			1150	17.99		
965.58	3.17			1200	8.30		

Table 4  
Molecular simulation results for JT inversion of the mixtures, this work.

$T / \text{K}$	$p / \text{MPa}$	$T / \text{K}$	$p / \text{MPa}$	$T / \text{K}$	$p / \text{MPa}$	$T / \text{K}$	$p / \text{MPa}$
methane + carbon dioxide		methane + ethane		nitrogen + methane		methane +	
275	40.30	275	29.10	125	0.80	carbon dioxide +	
350	58.68	350	45.14	200	31.28	nitrogen	
425	68.17	425	53.33	275	43.44	200	22.87
500	70.13	500	58.24	350	46.36	250	39.76
575	66.90	575	58.26	425	42.24	300	51.44
650	63.22	625	57.86	500	37.35	350	57.41
725	55.81	700	55.53	575	28.46	425	59.35
800	45.20	775	48.55	650	17.46	500	58.68
875	34.86	850	40.73	methane +		575	51.29
950	23.07	925	33.50	carbon dioxide +		650	43.62
methane +		950	29.86	ethane +		725	30.74
ethane +		1050	16.44	275	31.62	800	21.71
nitrogen +				350	49.72	875	15.03
200	17.46			425	60.60		
275	38.53			500	65.13		
350	48.64			575	65.15		
425	52.45			625	62.31		
500	51.80			700	59.16		
575	48.77			775	52.53		
650	42.27			850	45.07		
725	35.46			925	35.76		
800	25.26			1000	25.69		

## List of Figures

- 1 Joule-Thomson inversion curves of two pure fluids. Simulation:  
● methane, taken from [25], ■ carbon dioxide, taken from [25]; EOS: - - - DDMIX [18,19], ... SUPERTRAPP [20], -.- BACKONE [23], — GERG-2004 [24]. 23
- 2 Joule-Thomson inversion curves of two pure fluids. Simulation:  
● nitrogen, this work, ■ ethane, this work; EOS: - - - DDMIX [18,19], ... SUPERTRAPP [20], -.- BACKONE [23], — GERG-2004 [24]. 24
- 3 Deviation plots for Joule-Thomson inversion of the pure fluids. The baselines represent GERG-2004 [24]. Simulation: ●; EOS: - - - DDMIX [18,19], ... SUPERTRAPP [20], -.- BACKONE [23]; Reference EOS: — Setzmann and Wagner [13] (methane), Span et al. [14] (nitrogen), Span and Wagner [15] (carbon dioxide) and Friend et al. [16] (ethane). 25
- 4 Joule-Thomson inversion curves of two equimolar mixtures. Simulation: ● methane + carbon dioxide, this work, ■ nitrogen + methane, this work; EOS: - - - DDMIX [18,19], ... SUPERTRAPP [20], -.- BACKONE [23], — GERG-2004 [24]. 26
- 5 Joule-Thomson inversion curve of two equimolar mixtures. Simulation: ● methane + ethane, this work, ■ methane + carbon dioxide + nitrogen, this work; EOS: - - - DDMIX [18,19], ... SUPERTRAPP [20], -.- BACKONE [23], — GERG-2004 [24]. 27

- 6 Joule-Thomson inversion curve of two equimolar mixtures.  
Simulation: ● methane + carbon dioxide + ethane, this work,  
■ methane + ethane + nitrogen, this work; EOS: - - - DDMIX  
[18,19], ... SUPERTRAPP [20], -.-.- BACKONE [23], —  
GERG-2004 [24]. 28
- 7 Deviation plots for Joule-Thomson inversion of the binary  
mixtures. The baselines represent GERG-2004 [24]. Simulation:  
●; EOS: - - - DDMIX [18,19], ... SUPERTRAPP [20], -.-.-  
BACKONE [23]. 29
- 8 Deviation plots for Joule-Thomson inversion of the ternary  
mixtures. The baselines represent GERG-2004 [24]. Simulation:  
●; EOS: - - - DDMIX [18,19], ... SUPERTRAPP [20], -.-.-  
BACKONE [23]. 30

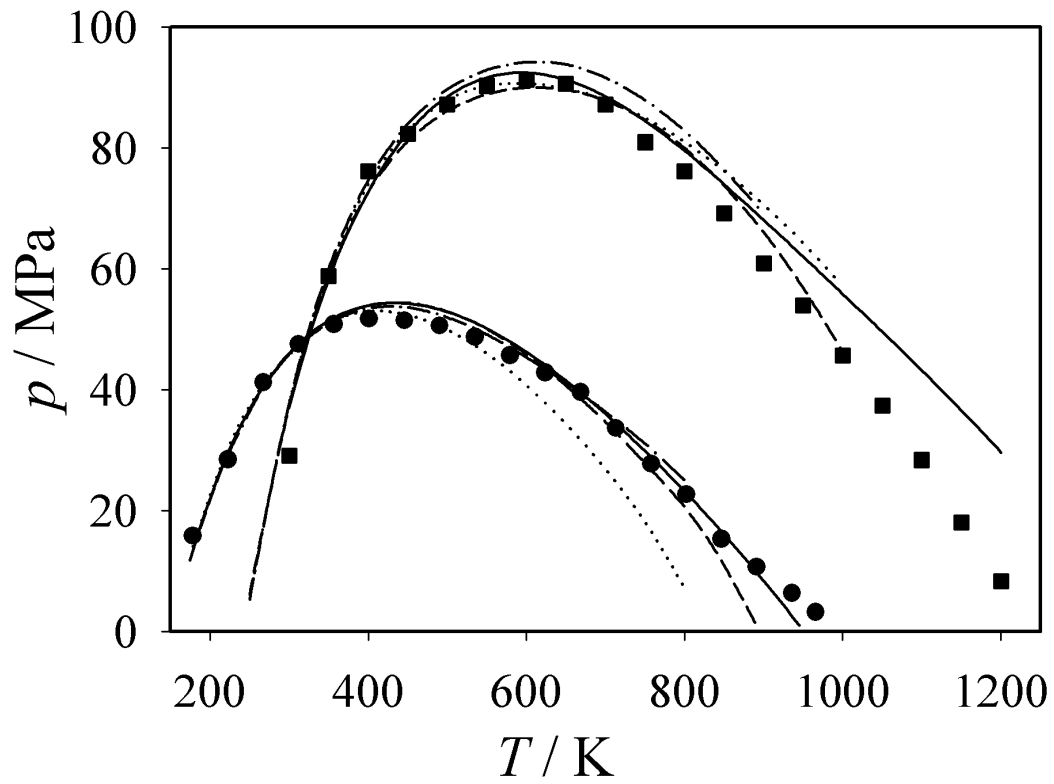


Fig. 1. Vrabc et al.

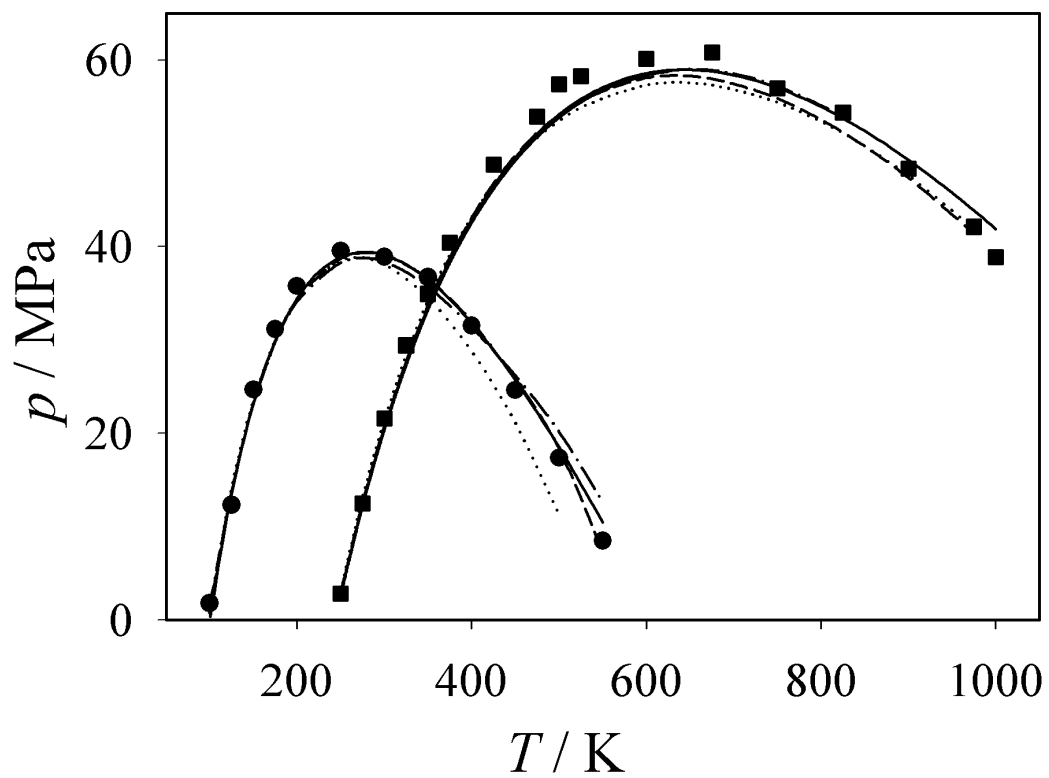


Fig. 2. Vrabc et al.



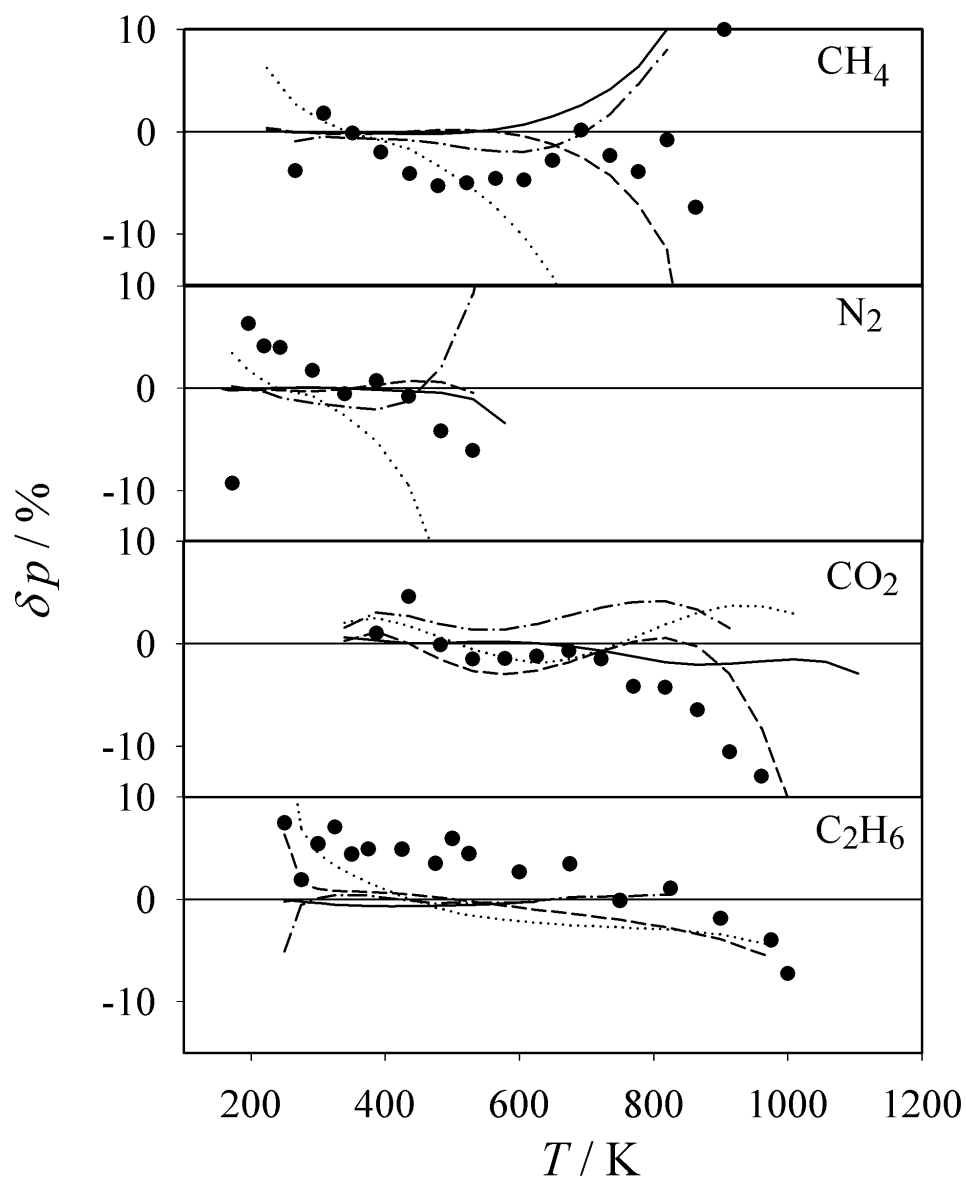


Fig. 3. Vrabec et al.

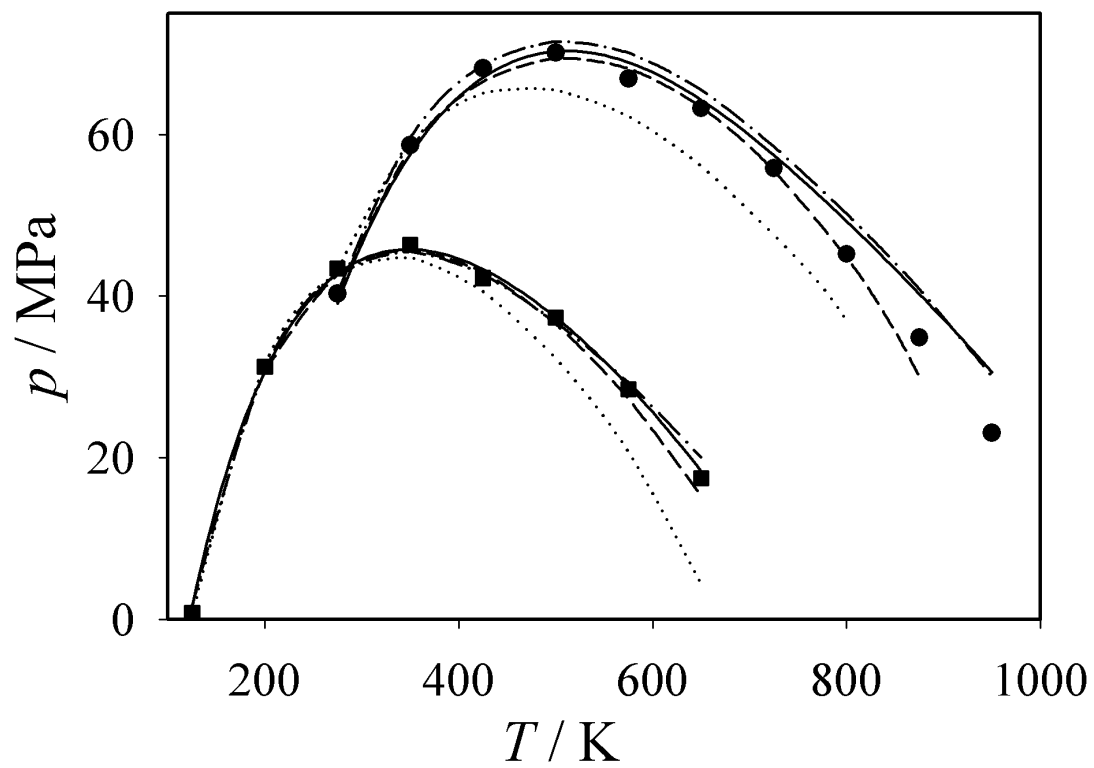


Fig. 4. Vrabc et al.

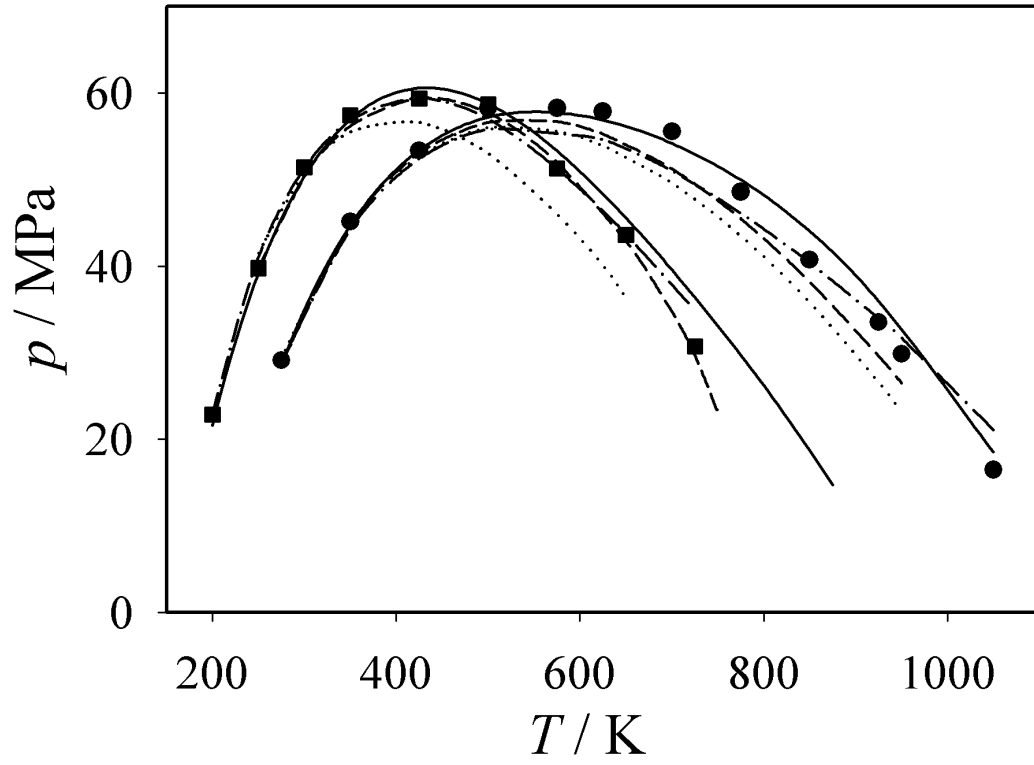


Fig. 5. Vrabc et al.

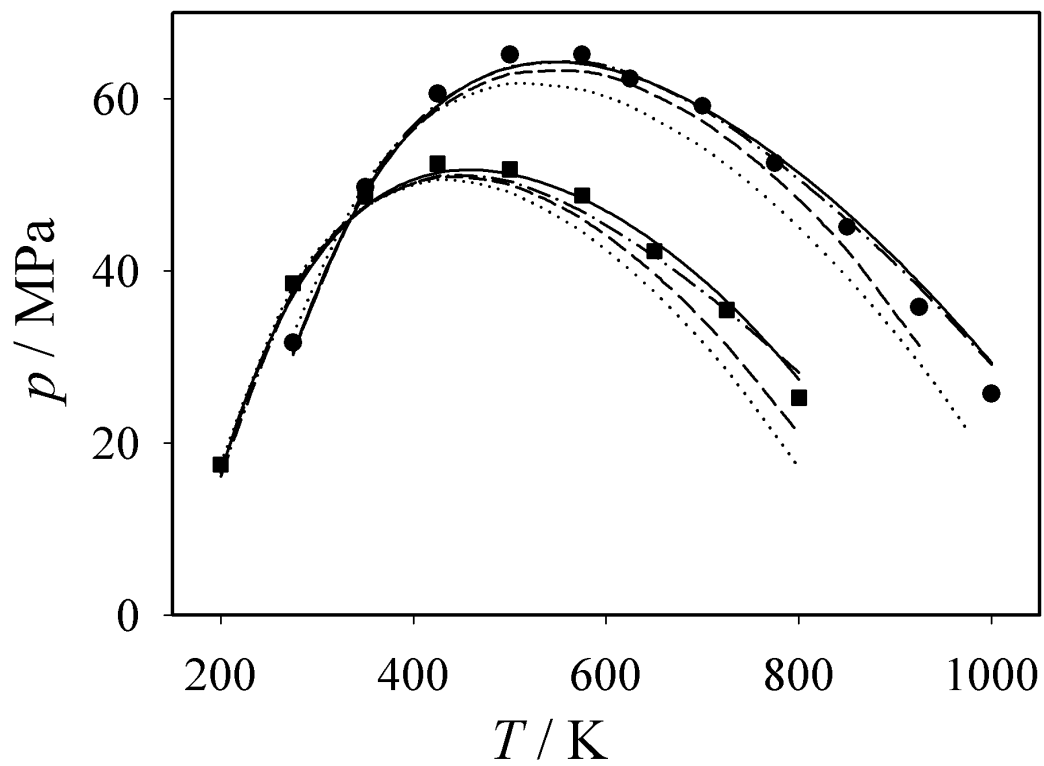


Fig. 6. Vrabec et al.

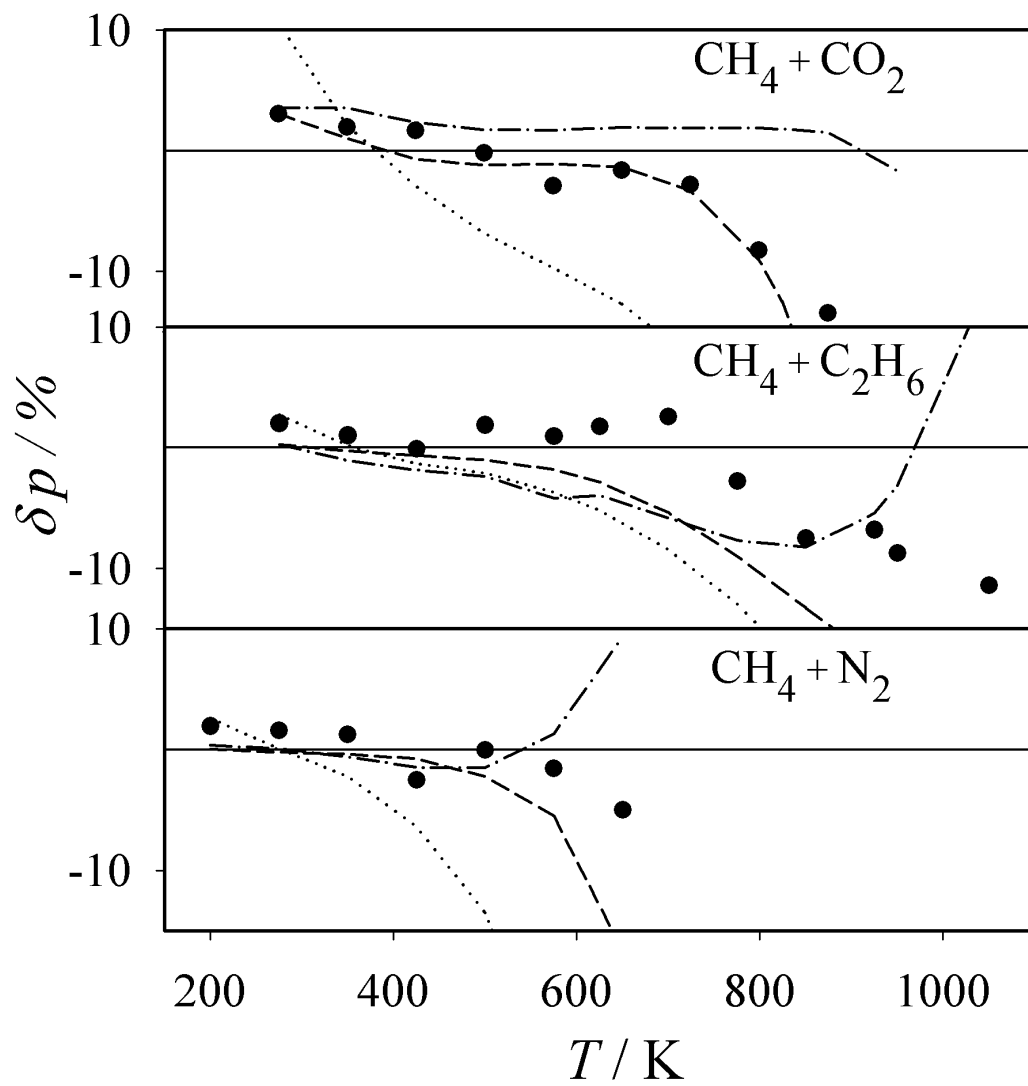


Fig. 7. Vrabec et al.

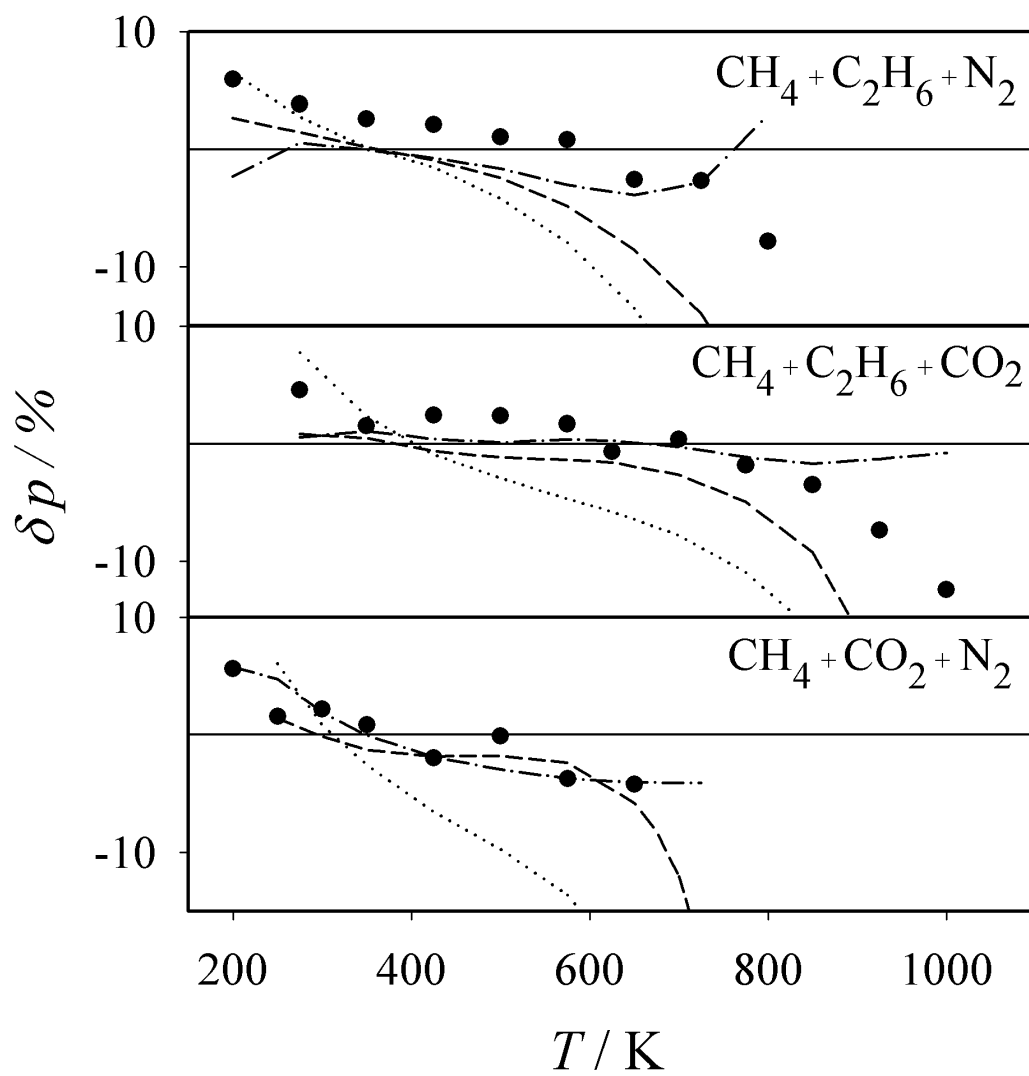


Fig. 8. Vrabc et al.

# Joule-Thomson inversion curves of mixtures by molecular simulation in comparison to advanced equations of state: natural gas as an example

Jadran Vrabec\*    Ashish Kumar    Hans Hasse

*Institut für Technische Thermodynamik und Thermische Verfahrenstechnik,  
Universität Stuttgart, D-70550 Stuttgart, Germany*

---

## Abstract

Molecular modelling and simulation as well as four equations of state (EOS) are applied to natural gas mixtures regarding Joule-Thomson (JT) inversion. JT inversion curves are determined by molecular simulation for six different natural gas mixtures consisting of Methane, Nitrogen, Carbon Dioxide and Ethane. These components are also regarded as pure fluids, leading to a total of ten studied systems. The results are compared to four advanced mixture EOS: DDMIX, SUPERTRAPP, BACKONE and the recent GERG-2004 Wide-Range Reference EOS. It is found that molecular simulation is competitive with state-of-the-art EOS in predicting JT inversion curves. The molecular based approaches (simulation and BACKONE) are superior to DDMIX and SUERTRAPP.

*Key words:*

---

## 1 Introduction

Due to the eminent importance of natural gas, knowledge on its thermodynamic behaviour and appropriate property models are of great interest. A property often

---

\* Corresponding author, Tel.: +49-711/685-66107, Fax: +49-711/685-66140  
*Email address:* vrabec@itt.uni-stuttgart.de (Jadran Vrabec).  
*URL:* www.itt.uni-stuttgart.de (Jadran Vrabec).

needed for applications of natural gases is the adiabatic (or isenthalpic) Joule-Thomson (JT) coefficient  $\mu$ , which is defined as the derivative of the temperature  $T$  with respect to the pressure  $p$  at constant enthalpy  $h$  and constant composition  $\underline{x}$

$$\mu = \left( \frac{\partial T}{\partial p} \right)_{h, \underline{x}}, \quad (1)$$

or, using basic thermodynamics relations,

$$\mu = - \frac{1}{c_p} \left( \frac{\partial h}{\partial p} \right)_{T, \underline{x}}, \quad (2)$$

where  $c_p$  is the isobaric heat capacity. The JT inversion curve, connecting all state points with  $\mu=0$ , divides the pressure-temperature plane into two regions. In the lower region,  $\mu$  is positive so that an adiabatic expansion leads to a decrease in temperature. In the upper region,  $\mu$  is negative. It can be shown that the cooling effect is maximized if an expansion starts from the inversion pressure.

The experimental determination of a fluid's JT inversion curve demands precise measurements of volumetric and caloric properties over a broad range of temperature and pressure. Temperature and pressure reach up to a five-fold and twelve-fold of their critical values, respectively. Experimental JT inversion curve data are therefore scarce, sometimes unreliable [1], and mostly available only for pure fluids [2]. An example for mixture data is the work of Charnley et al. [3] on e.g. Carbon Dioxide + Nitrous Oxide, Carbon Dioxide + Ethylene. A good overview over experimental data is given in [2].

For industrial applications there is a need for a proper representation and also for the prediction of JT data, as it is not feasible to measure it for all relevant and



often very different blends. Some authors, e.g., Miller [7] or Gunn et al. [8], have proposed direct representations of the JT inversion curve, which have hardly any predictive power. Significantly more valuable are proper equations of state (EOS) that contain much more thermodynamic information and are valid for a broad range of state points. Thus, extensive efforts are made to use EOS for predictions of the JT inversion curve. Examples for the use of cubic EOS are modified versions of Peng-Robinson [9,10], Redlich-Kwong [9,11], Soave-Redlich-Kwong [10], Patel-Teja [9] or other cubic EOS [12] with varying parameter functions. Unfortunately, cubic EOS are usually unreliable, especially in the high temperature region, where they often fail completely.

Among mixtures, natural gases are the ones that were investigated most extensively both experimentally and theoretically so that very reliable thermodynamic data and models are available. Therefore, natural gases are excellent test systems to validate thermodynamic models for mixtures.

Natural gas from the rig is a mixture of typically seventeen components (containing Methane, Nitrogen, Carbon Dioxide, Ethane, Propane) [4], but usually its main component is Methane [5,6]. As a natural product, it has a great variability in composition and, depending on conditions in the formation process, considerable quantities of Nitrogen (up to 60 mole %), Carbon Dioxide (up to mole 50 %) or Ethane (up to mole 20 %) are encountered [5].

For a number of pure natural gas components, reference EOS have been developed based on a vast experimental data set considering different thermodynamic properties, e.g., Methane [13], Nitrogen [14], Carbon Dioxide [15] and Ethane [16]. Reference EOS have an empirical background, but they are parameterized extremely carefully, taking also available experimental JT coefficients into ac-

count. Hence, they are regarded in this work as the best available information.

For mixtures, the National Institute of Standards and Technology (NIST) [17] provided two classical phenomenological EOS, i.e. DDMIX [18,19] and SUPERTRAPP [20]. DDMIX is an implementation of the NIST extended corresponding states model for mixtures, whereas SUPERTRAPP is based on both a modified Peng-Robinson EOS and the NIST extended corresponding states model for mixtures. Both were parameterized to experimental pure substance and mixture data. Particularly SUPERTRAPP is often used in the literature as a property model for designing cooling cycles with mixed coolants, e.g. [21,22].

There are also physically based EOS that take the different molecular interactions, like dispersion or polarity, explicitly into account; an example is the BACKONE-EOS [23]. Such EOS can be parameterized for real substances with a very small experimental data set, e.g. a few vapour-liquid equilibrium data points, as they have a good predictive power. Furthermore, the GERG-2004 Wide-Range Reference EOS [24] has become available recently, which applies the concept of reference EOS to mixtures. Here too, a vast set of experimental data, both pure substance and mixture, was used for the development.

Molecular modelling and simulation offers an interesting alternative approach for predicting thermodynamic properties. Instead of describing those macroscopic properties directly, the intermolecular interactions are described. Previous work from our group [25] has demonstrated the good predictive power of molecular models for JT inversion curves for different pure fluids, but also for the mixture air which has been modelled as a ternary system containing Nitrogen, Oxygen and Argon. The objective of the present paper is to validate the predictive power of available molecular models by comparing the results to the four advanced EOS

mentioned above using different natural gas mixtures and their most important pure components regarding JT inversion.

## 2 Molecular model and simulation method

Most publications on JT inversion curves by molecular simulation are based on the spherical Lennard-Jones (LJ) model [26,27,28,29], which is appropriate only for simple molecules like Methane and the noble gases. However, this simple potential model is well suited to further develop molecular simulation techniques for determining JT inversion as reliable simulation data is available for comparison. E.g., Colina et al. [30] have chosen two different routes, i.e. via compressibility [31,32] or via thermal expansivity [33], to simulate the JT inversion curve. Work on more complex fluids is still scarce, examples are Chacín et al. [34] (Carbon Dioxide), Lísal et al. [35] (R32), Kristóf et al. [36] (Hydrogen Sulphide), or a recent work of our group [25] dealing with fifteen different pure substances (including Methane, Carbon Dioxide, R134a, R143a, R152a, etc.) and the mixture air.

The effective 2CLJQ pair potential was used as molecular model here to describe the intermolecular interactions in all cases. This can be done, as only the four most common components Methane, Nitrogen, Carbon Dioxide and Ethane were considered, being well suited for this modelling approach. The 2CLJQ potential is composed out of two identical Lennard-Jones sites a distance  $L$  apart (2CLJ) and a point quadrupole with momentum  $Q$  placed in the geometric centre of the molecule oriented along the molecular axis

$$u_{2CLJQ}(\mathbf{r}_{ij}, \boldsymbol{\omega}_i, \boldsymbol{\omega}_j, L, Q) = u_{2CLJ}(\mathbf{r}_{ij}, \boldsymbol{\omega}_i, \boldsymbol{\omega}_j, L) + u_Q(\mathbf{r}_{ij}, \boldsymbol{\omega}_i, \boldsymbol{\omega}_j, Q), \quad (3)$$

wherein  $u_{2\text{CLJ}}$  is the contribution of the four Lennard-Jones interactions

$$u_{2\text{CLJ}}(\mathbf{r}_{ij}, \boldsymbol{\omega}_i, \boldsymbol{\omega}_j, L) = \sum_{a=1}^2 \sum_{b=1}^2 4\epsilon \left[ \left( \frac{\sigma}{r_{ab}} \right)^{12} - \left( \frac{\sigma}{r_{ab}} \right)^6 \right]. \quad (4)$$

The quadrupolar contribution  $u_Q$ , is given by [37]

$$u_Q(\mathbf{r}_{ij}, \boldsymbol{\omega}_i, \boldsymbol{\omega}_j, Q) = \frac{3}{4} \frac{Q^2}{|\mathbf{r}_{ij}|^5} f_Q(\boldsymbol{\omega}_i, \boldsymbol{\omega}_j). \quad (5)$$

Herein,  $\mathbf{r}_{ij}$  is the centre-centre distance vector of two molecules  $i$  and  $j$ ,  $r_{ab}$  is one of the four Lennard-Jones site-site distances;  $a$  counts the two sites of molecule  $i$ ,  $b$  counts those of molecule  $j$ . The vectors  $\boldsymbol{\omega}_i$  and  $\boldsymbol{\omega}_j$  represent the orientations of the two molecules  $i$  and  $j$ .  $f_Q$  is a trigonometric function depending on these molecular orientations, cf. [37]. The Lennard-Jones parameters  $\sigma$  and  $\epsilon$  represent size and energy, respectively. 2CLJQ models have the four state independent model parameters  $\sigma$ ,  $\epsilon$ ,  $L$ , and  $Q$ , which have been adjusted to experimental vapour pressure, bubble density and critical temperature in a recent work of our group [38]. All pure substance parameters are given in Table 1. The spherical non-polar LJ model for Methane is a limiting case of 2CLJQ models, where  $L = 0$  and  $Q = 0$ .

To perform simulations of mixtures, a molecular mixture model is needed. On the basis of pairwise additive pure fluid models, molecular modelling of mixtures reduces to modelling interactions between unlike molecules. Here, the modified Lorentz-Berthelot combining rule with one adjustable binary interaction parameter  $\xi$  was used for each unlike Lennard-Jones interaction

$$\sigma_{\text{AB}} = \frac{\sigma_{\text{A}} + \sigma_{\text{B}}}{2}, \quad (6)$$

$$\epsilon_{\text{AB}} = \xi \cdot \sqrt{\epsilon_{\text{A}} \cdot \epsilon_{\text{B}}}. \quad (7)$$

The state independent parameter  $\xi$  was adjusted to one experimental vapour pressure of each binary mixture in prior work of our group [39,40,41]. Table 2 reports the six binary parameters of the quaternary natural gas mixture model. The unlike quadrupolar interactions are treated in a physically straightforward way, following the laws of electrostatics without any binary parameters. It should be pointed out, that exclusively experimental VLE data were used in the parameterization of the molecular mixture model, but no caloric data.

For the calculation of JT inversion curves on the basis of a given model by molecular simulation, several methods have been proposed in the literature [31,32,33,42,43]. Here, as in prior work [25], an intuitive and straightforward method was used. To calculate one JT inversion pressure  $p$  for a given temperature  $T$ , a series of simulations, generally from 5 to 10, were made around the expected result, covering typically a rather large pressure range of 20 MPa. In these simulations, the enthalpy  $h$  and its partial derivative with respect to pressure  $(\partial h/\partial p)_{T,\underline{x}}$  were calculated. Both data sets were fitted simultaneously by a second order polynomial vs. pressure at that particular temperature. The inversion pressure corresponds simply to the minimum value of enthalpy, i.e. the minimum of that quadratic fit.

Molecular dynamics simulations were performed in the isobaric-isothermal ( $NpT$ ) ensemble, using Andersen's barostat [44] and isokinetic velocity scaling [45] for thermostating. After 6 000 equilibration time steps, the residual enthalpy [46]

$$h^{res} = \frac{1}{N} \cdot \left\{ \left\langle \sum_{i=1}^N \sum_{j>i}^N u_{2CLJQ}(\mathbf{r}_{ij}, \boldsymbol{\omega}_i, \boldsymbol{\omega}_j, L, Q) \right\rangle + p \langle V \rangle \right\} - k_B T, \quad (8)$$

was averaged over 200 000 time steps, where the first term indicates the simulation average over the intermolecular potential energy and  $\langle V \rangle$  is the average of the extensive volume. The partial derivative was obtained by a fluctuation

expression [47]

$$\left(\frac{\partial h^{res}}{\partial p}\right)_{T,\underline{x}} = \frac{1}{N} \cdot \left\{ \frac{1}{k_B T} \cdot [\langle V \rangle \langle H^{res} \rangle - \langle V H^{res} \rangle] + \langle V \rangle \right\}, \quad (9)$$

where  $H^{res}$  is the extensive residual enthalpy. The ideal part of the enthalpy is not relevant, as it is not pressure dependent.

Depending on the density of the state point, the membrane mass parameter  $M$  of Andersen's barostat [44] was chosen from  $10^{-20}$  to  $10^{-15}$  kg/m<sup>4</sup>. The intermolecular interactions were evaluated explicitly up to a cut-off radius of  $r_c = 5\sigma$  and standard long range corrections were used for the Lennard-Jones interaction, employing angle averaging as proposed by Lustig [48]. Long-range corrections for the quadrupolar interaction are not needed since they disappear. A total number of  $N = 1372$  molecules were initially placed in a fcc lattice configuration into a cubic simulation box, where the density of the system was chosen close to that expected from an EOS, if available, otherwise estimates were used.

### 3 Results

JT inversion curves are compared for six different systematically chosen gas mixtures consisting of the four main natural gas components Methane, Nitrogen, Carbon Dioxide and Ethane. Firstly, the three Methane containing binary systems that can be formed from these four components were studied at equimolar composition, where the highest effect of mixing can be expected. Following this, secondly, all three ternary systems containing Methane were studied, again at equimolar composition, i.e. with a mole fraction  $x_i = 1/3$  throughout. Finally, also the four pure fluids were investigated.

Simulation results for pure Methane and Carbon Dioxide were taken from prior work [25], but for Nitrogen and Ethane as well as for all mixtures new simulation results are presented. Tables 3 and 4 compile the full simulation data set. The statistical uncertainties of this data are estimated to be in the order of 1 MPa. This translates into a relative error of around 2 % for medium temperatures, but the relative errors are considerably larger at extremely low and high temperatures, where the inversion pressure approaches zero.

For all systems the results for the JT inversion curves from molecular simulation are compared to the four mixture EOS, i.e. DDMIX [18,19], SUPERTRAPP [20], BACKONE-EOS [23] and GERG-2004 [24]. The pure substance results are additionally compared to reference EOS using the program package REFPROP [49]. All results are presented in pressure-temperature diagrams as well as in deviation plots.

### *3.1 Pure components*

Figures 1 and 2 present the JT inversion curves of the pure fluids, which were grouped to achieve a good visibility. In these Figures, it can be seen that the results from the different methods qualitatively agree. Especially in the low temperature region of the JT inversion curves, they are often undistinguishable in these absolute plots. Significant deviations, however, occur for higher temperatures. For a more detailed discussion, the deviation plots in Figure 3 are more suited, where the baselines represent GERG-2004. It should be pointed out that in Figure 3 additionally the pure substance reference EOS [13,14,15,16] results are shown. GERG-2004 agrees with the reference EOS within less than about 3 % throughout, except for Methane at high temperatures. DDMIX and BACKONE

agree roughly equally well to GERG-2004 as well as the simulation data, often with the same trends. Generally, these results lie within a band of about 5 %, larger deviations are found particularly at high temperatures. BACKONE yields mostly higher results for high temperatures than GERG-2004, whereas DDMIX tends to yield lower values. Significantly worse is SUPERTRAPP which yields negative deviations of more than 10 % in large parts of the high temperature range of Methane and Nitrogen.

### 3.2 *Mixtures*

Figures 4 to 6 present the JT inversion curves for the six equimolar binary and ternary mixtures, which are again grouped to achieve good visibility. As for the pure fluids, the qualitative agreement between the different studied models is observed throughout. The agreement between all models is almost always excellent for low temperatures, but significant deviations are found in the high temperature region. Compared to the pure substances the spread between the different models is larger. Also here, the results can better be resolved in deviation plots, where the baselines were again chosen to represent GERG-2004 data. Figure 7 shows the binary and Figure 8 the ternary cases. Simulation data and GERG-2004 agree also for mixtures usually within 5 %, larger relative deviations are found for very high temperatures. BACKONE shows a comparable performance. It yields systematically higher values at strongly elevated temperatures and a better agreement with GERG-2004 than DDMIX and SUPERTRAPP. These two EOS show poorer results throughout, which are always too low by more than 10 % at high temperatures. SUPERTRAPP yields the largest deviations in all cases.



GERG-2004 was taken as a reference here as the broadest possible experimental data set was taken for its parameterization. This is confirmed by the fact that GERG-2004 data lies almost always in between the remaining results. Comparing it to the reference EOS for pure fluids, which were individually fitted including JT inversion data, an uncertainty of only about 3 % has to be assumed, except for methane at high temperatures.

#### 4 Conclusion

In this work, results from molecular modelling and simulation were compared to four advanced mixture EOS regarding JT inversion curves of natural gas mixtures. With a focus on the four most important components Methane, Nitrogen, Carbon Dioxide and Ethane, six different equimolar binary and ternary mixtures were selected systematically. As a reference and for completeness, the four components were also regarded as pure fluids. The comparison shows that molecular modelling and simulation is competitive with the most state-of-the-art EOS in predicting JT inversion curves. This approach has a similar performance as BACKONE, which is based on molecular simulation data itself. DDMIX and particularly SUPERTRAPP are less reliable.

It can be stated that for other mixtures, where no such elaborate EOS are available, that molecular modelling and simulation is the method of choice to predict JT inversion.

## 5 Acknowledgment

We gratefully acknowledge financial support by Deutsche Forschungsgemeinschaft, Schwerpunktprogramm 1155.

## References

- [1] Hiza MJ, Kidnay AJ, Miller RC. Equilibrium Properties of Fluid Mixtures. New York: IFI/Plenum 1975.
- [2] Perry RH, Green DW, Editors. Perry's Chemical Engineers' Handbook. 7th Ed. New York: McGraw-Hill 1997.
- [3] Charnley A, Rowlinson JS, Sutton JR, Townley JR. The Isothermal Joule-Thomson Coefficient of Some Binary Gas Mixtures. Proceedings of the Royal Society of London. Series A, Mathematical and Physical Sciences 1955;230:354-358.
- [4] Bergman DF, Tek MR, Katz DL. Retrograde condensation in natural gas pipelines, Am Gas Assoc, Pipeline Res Committee L22277, Project PR 26-29, 1975.
- [5] Technical Note 412, United States Department of the Interior, Bureau of Land Management, Analyses of Natural Gases 1998-2001.  
<http://www.blm.gov/nstc/library/pdf/TN412.pdf>.
- [6] Ginter D, Simchick C, Schlakker J. Durability of Catalytic Combustion Systems. APPENDIX VI: Variability in Natural Gas Fuel Composition and Its Effects on the Performance of Catalytic Combustion Systems, California Energy Commission 2001.
- [7] Miller DG. Joule-Thomson inversion curve corresponding state, and simpler equations of state. Ind Eng Chem Fundam 1970;9:585-589.
- [8] Gunn RD, Chueh PL, Prausnitz JM. Inversion temperatures and pressures for cryogenic gases and their mixtures. Cryogenics 1966;6:324-329.
- [9] Matin NS, Haghighi B. Calculation of the Joule-Thomson inversion curves from cubic equations of state. Fluid Phase Equilib 2000;175:273-284.
- [10] Haghighi B, Laee MR, Matin NS. A comparison among five equations of state in predicting the inversion curve of some fluids. Cryogenics 2003;43:393-398.
- [11] Juris K, Wenzel LA. A study of inversion curves. AIChE J 1972;18:684-688.

- [12] Haghghi B, Laee MR, Husseindokht MR, Matin NS. Prediction of Joule-Thomson Inversion Curves by the Use of Equation of State, *J Ind Eng Chem* 2004;10:316-320.
- [13] Setzmann U, Wagner W. A new equation of state and tables of the thermodynamic properties for methane covering the range from the melting line to 625 K at pressures up to 1000 MPa. *J Phys Chem Ref Data* 1991;20:1061-1155.
- [14] Span R, Lemmon EW, Jacobsen RT, Wagner W, Yokozeki A. A reference equation of state for the thermodynamic properties of nitrogen for temperatures from 63.151 to 1000 K and pressures to 2200 MPa. *J Phys Chem Ref Data* 2000;29:1361-1433.
- [15] Span R, Wagner W. A new equation of state for carbon dioxide covering the fluid region from the triple-point temperature to 1100 K at pressures up to 800 MPa. *J Phys Chem Ref Data* 1996;25:1509-1596.
- [16] Friend DG, Ingham H, Ely JF. Thermophysical properties of ethane. *J Phys Chem Ref Data* 1991;20:275-347.
- [17] <http://www.nist.gov/>.
- [18] Ely JF, Magee JW, Haynes WM. NBS standard reference database 14, DDMIX, Version 9,06, NIST, Boulder, Colorado 1989.
- [19] Ely JF. A Predictive, Exact Shape Factor Extended Corresponding States Model for Mixtures. *Adv Cryog Eng* 1990;35:1511.
- [20] James EF, Huber MI. NIST Thermodynamic Properties of Hydrocarbon Mixtures Database (SUPERTRAPP). US Department of Commerce, National Institute of Standards and Technology 1992.
- [21] Maytal B-Z, Nellis GF, Klein SA, Pfothenhauer JM. Elevated-pressure mixed-coolants Joule-Thomson cryocooling. *Cryogenics* 2006;46:55-67.
- [22] Huang H, Spadaccini LJ, Sobel DR. Fuel-Cooled Thermal Management for Advanced Aeroengines, *J Eng Gas Turbines Power* 2004;126:284-293.
- [23] Wendland M, Saleh B, Fischer J. Accurate Thermodynamic Properties from the BACKONE Equation for the Processing of the Natural Gas. *Energy and Fuels* 2004;18:938-951.
- [24] Kunz O, Klimeck R, Wagner W, Jaeschke M. The GERG-2004 Wide-Range Reference Equation of State for Natural Gases and Other Mixtures. To be published as GERG Technical Monograph. *Fortschr.-Ber. VDI, VDI-Verlag, Düsseldorf*, 2006.
- [25] Vrabec J, Kedia GK, Hasse H. Prediction of Joule-Thomson inversion curves for pure fluids and one mixture by molecular simulation. *Cryogenics* 2005;45:253-258.
- [26] Bessières D, Randzio SL, Piñeiro MM, Lafitte T, Daridon J-L. A Combined Pressure-controlled Scanning Calorimetry and Monte Carlo Determination of the Joule-Thomson Inversion Curve. Application to Methane. *J Phys Chem B* 2006;110:5659-5664.

- [27] Heyes DM, Llaguno CT. Computer simulation and equation of state study of the Boyle and inversion temperature of simple fluids. *Chem Phys* 1992;168:61-68.
- [28] Colina CM, Muller EA. Molecular Simulation of Joule-Thomson Inversion Curves. *Int J Thermophys* 1999;20:229-235.
- [29] Kioupis LI, Arya G, Maginn EJ. Pressure-enthalpy driven molecular dynamics for thermodynamic property calculation II. Applications. *Fluid Phase Equilib* 2002;200:93-110.
- [30] Colina CM, Lísal M, Siperstein FR, Gubbins KE. Accurate  $CO_2$  Joule-Thomson inversion curve by molecular simulations. *Fluid Phase Equilib* 2002;202:253-262.
- [31] Colina CM, Müller EA. Molecular Simulation of Joule-Thomson Inversion Curves. *Int J Thermophys* 1999;20:229-235.
- [32] Colina CM, Müller EA. Joule-Thomson inversion curves by molecular simulation. *Mol Sim* 1997;19:237-246.
- [33] Lagache M, Ungerer P, Boutin A, Fuchs AH. Prediction of thermodynamic derivative properties of fluids by Monte Carlo simulation. *Phys Chem Chem Phys* 2001;3:4333-4339.
- [34] Chacín A, Vázquez JM, Muller EA. Molecular Simulation of Joule-Thomson Inversion Curve of carbon dioxide. *Fluid Phase Equilib* 1999;165:147-155.
- [35] Lísal M, Smith WR, Aim K. Direct molecular-level Monte Carlo simulation of Joule-Thomson processes. *Mol Phys* 2003;101:2875-2884.
- [36] Kristóf T, Rutkai G, Merényi L, Liszi J. Molecular simulation of the Joule-Thomson inversion curve of the hydrogen sulphide. *Mol Phys* 2005;103:537-545.
- [37] Gray CG, Gubbins KE. Theory of molecular fluids. Fundamentals. Oxford: Clarendon Press 1984.
- [38] Vrabec J, Stoll J, Hasse H. A set of molecular models for symmetric quadrupolar fluids. *J Phys Chem B* 2003;105:12126-12133.
- [39] Stoll J, Vrabec J, Hasse H. Vapour-Liquid equilibria of mixtures containing nitrogen, oxygen, carbon dioxide, and ethane. *AIChE J* 2003;49:2187-2198.
- [40] Vrabec J, Stoll J, Hasse H. Molecular models of unlike interactions in fluid mixtures. *Mol Sim* 2005;31:215-221.
- [41] Huang YL. Systematic investigation of vapor-liquid equilibria of binary mixtures on the basis of polar two-center Lennard-Jones models, MSc thesis, University of Stuttgart 2005.
- [42] Colina C, Muller EA. Joule-Thomson inversion curves by molecular simulation. *Mol Sim* 1997;19:237-246.

- [43] Kioupis LI, Maginn EJ. Pressure-enthalpy driven molecular dynamics for thermodynamic property calculation I. Methodology. *Fluid Phase Equilib* 2002;200:75-92.
- [44] Andersen HC. Molecular dynamics simulations at constant pressure and/or temperature. *J Chem Phys* 1980;72:2384-2393.
- [45] Allen MP, Tildesley DJ. *Computer Simulation of Liquids*. Oxford: Clarendon Press 1987.
- [46] Heermann DW. *Computer Simulation Methods in Theoretical Physics*. Springer-Verlag, Berlin 1986.
- [47] Hill TL. *Statistical Mechanics*. McGraw-Hill Book Company. New York 1956.
- [48] Lustig R. Angle-average for the powers of the distance between two separated vectors. *Molec Phys* 1988;65:175-179.
- [49] REFPROP, NIST Standard Reference Database 23, Version 7.0:2002.

Table 1  
Parameters of pure fluid molecular models, taken from [38].

Fluid	$\sigma/\text{\AA}$	$(\epsilon/k_B)/\text{K}$	$L/\text{\AA}$	$Q/\text{D}\text{\AA}$
Methane	3.7281	148.55	-	-
Nitrogen	3.3211	34.897	1.0464	1.4397
Carbon Dioxide	2.9847	133.22	2.4176	3.7938
Ethane	3.4896	136.99	2.3762	0.8277

Table 2  
Binary interaction parameters, taken from [39,40,41].

Mixture	$\xi$
Methane + Carbon Dioxide	0.997
Methane + Ethane	0.958
Nitrogen + Methane	0.974
Nitrogen + Carbon Dioxide	0.962
Nitrogen + Ethane	0.954
Carbon Dioxide + Ethane	1.041

Table 3

Molecular simulation results for JT inversion of the pure components. Data for Methane and Carbon Dioxide was taken from [25], the remainder is from this work.

$T / \text{K}$	$p / \text{MPa}$	$T / \text{K}$	$p / \text{MPa}$	$T / \text{K}$	$p / \text{MPa}$	$T / \text{K}$	$p / \text{MPa}$
Methane		Nitrogen		Carbon Dioxide		Ethane	
178.26	15.83	100	1.81	300	29.05	250	2.83
222.83	28.43	125	12.31	350	58.80	275	12.50
267.39	41.22	150	24.68	400	76.09	300	21.58
311.96	47.53	175	31.13	450	82.32	325	29.42
356.52	50.83	200	35.78	500	87.16	350	34.94
401.09	51.73	250	39.54	550	90.27	375	40.45
445.65	51.44	300	38.88	600	91.31	425	48.80
490.22	50.58	350	36.72	650	90.62	475	53.93
534.78	48.73	400	31.55	700	87.16	500	57.38
579.35	45.68	450	24.62	750	80.94	525	58.28
623.91	42.81	500	17.37	800	76.09	600	60.14
668.48	39.56	550	8.48	850	69.18	675	60.82
713.04	33.62			900	60.87	750	56.97
757.61	27.73			950	53.96	825	54.34
802.17	22.68			1000	45.66	900	48.37
846.74	15.27			1050	37.35	975	42.13
891.30	10.68			1100	28.36	1000	38.86
935.87	6.32			1150	17.99		
965.58	3.17			1200	8.30		

Table 4  
Molecular simulation results for JT inversion of the mixtures, this work.

$T / \text{K}$	$p / \text{MPa}$	$T / \text{K}$	$p / \text{MPa}$	$T / \text{K}$	$p / \text{MPa}$	$T / \text{K}$	$p / \text{MPa}$
Methane + Carbon Dioxide		Methane + Ethane		Nitrogen + Methane		Methane +	
275	40.30	275	29.10	125	0.80	Carbon Dioxide +	
350	58.68	350	45.14	200	31.28	Nitrogen	
425	68.17	425	53.33	275	43.44	200	22.87
500	70.13	500	58.24	350	46.36	250	39.76
575	66.90	575	58.26	425	42.24	300	51.44
650	63.22	625	57.86	500	37.35	350	57.41
725	55.81	700	55.53	575	28.46	425	59.35
800	45.20	775	48.55	650	17.46	500	58.68
875	34.86	850	40.73	Methane +		575	51.29
950	23.07	925	33.50	Carbon Dioxide +		650	43.62
Methane +		950	29.86	Ethane +		725	30.74
Ethane +		1050	16.44	275	31.62	800	21.71
Nitrogen +				350	49.72	875	15.03
200	17.46			425	60.60		
275	38.53			500	65.13		
350	48.64			575	65.15		
425	52.45			625	62.31		
500	51.80			700	59.16		
575	48.77			775	52.53		
650	42.27			850	45.07		
725	35.46			925	35.76		
800	25.26			1000	25.69		



## List of Figures

- 1 Joule-Thomson inversion curves of two pure fluids. Simulation:  
● Methane, taken from [25], ■ Carbon Dioxide, taken from [25]; EOS: - - - DDMIX [18,19], ... SUPERTRAPP [20], -.-.- BACKONE [23], — GERG-2004 [24]. 21
- 2 Joule-Thomson inversion curves of two pure fluids. Simulation:  
● Nitrogen, this work, ■ Ethane, this work; EOS: - - - DDMIX [18,19], ... SUPERTRAPP [20], -.-.- BACKONE [23], — GERG-2004 [24]. 22
- 3 Deviation plots for Joule-Thomson inversion of the pure fluids. The baselines represent GERG-2004 [24]. Simulation: ●; EOS: - - - DDMIX [18,19], ... SUPERTRAPP [20], -.-.- BACKONE [23]; Reference EOS: — Setzmann and Wagner [13] (Methane), Span et al. [14] (Nitrogen), Span and Wagner [15] (Carbon Dioxide) and Friend et al. [16] (Ethane). 23
- 4 Joule-Thomson inversion curves of two equimolar mixtures. Simulation: ● Methane + Carbon Dioxide, this work, ■ Nitrogen + Methane, this work; EOS: - - - DDMIX [18,19], ... SUPERTRAPP [20], -.-.- BACKONE [23], — GERG-2004 [24]. 24
- 5 Joule-Thomson inversion curve of two equimolar mixtures. Simulation: ● Methane + Ethane, this work, ■ Methane + Carbon Dioxide + Nitrogen, this work; EOS: - - - DDMIX [18,19], ... SUPERTRAPP [20], -.-.- BACKONE [23], — GERG-2004 [24]. 25

- 6 Joule-Thomson inversion curve of two equimolar mixtures.  
Simulation: ● Methane + Carbon Dioxide + Ethane, this work, ■ Methane + Ethane + Nitrogen, this work; EOS: - - - DDMIX [18,19], ... SUPERTRAPP [20], -.- BACKONE [23], — GERG-2004 [24]. 26
- 7 Deviation plots for Joule-Thomson inversion of the binary mixtures. The baselines represent GERG-2004 [24]. Simulation: ●; EOS: - - - DDMIX [18,19], ... SUPERTRAPP [20], -.- BACKONE [23]. 27
- 8 Deviation plots for Joule-Thomson inversion of the ternary mixtures. The baselines represent GERG-2004 [24]. Simulation: ●; EOS: - - - DDMIX [18,19], ... SUPERTRAPP [20], -.- BACKONE [23]. 28

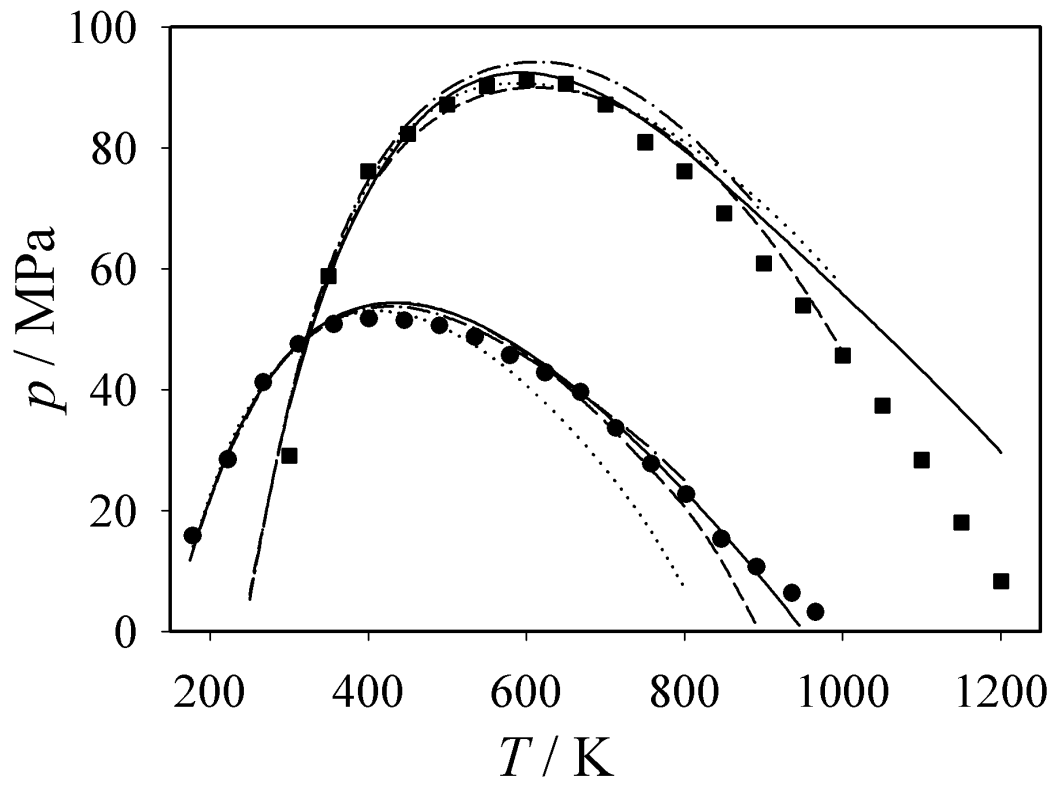


Fig. 1. Vrabc et al.

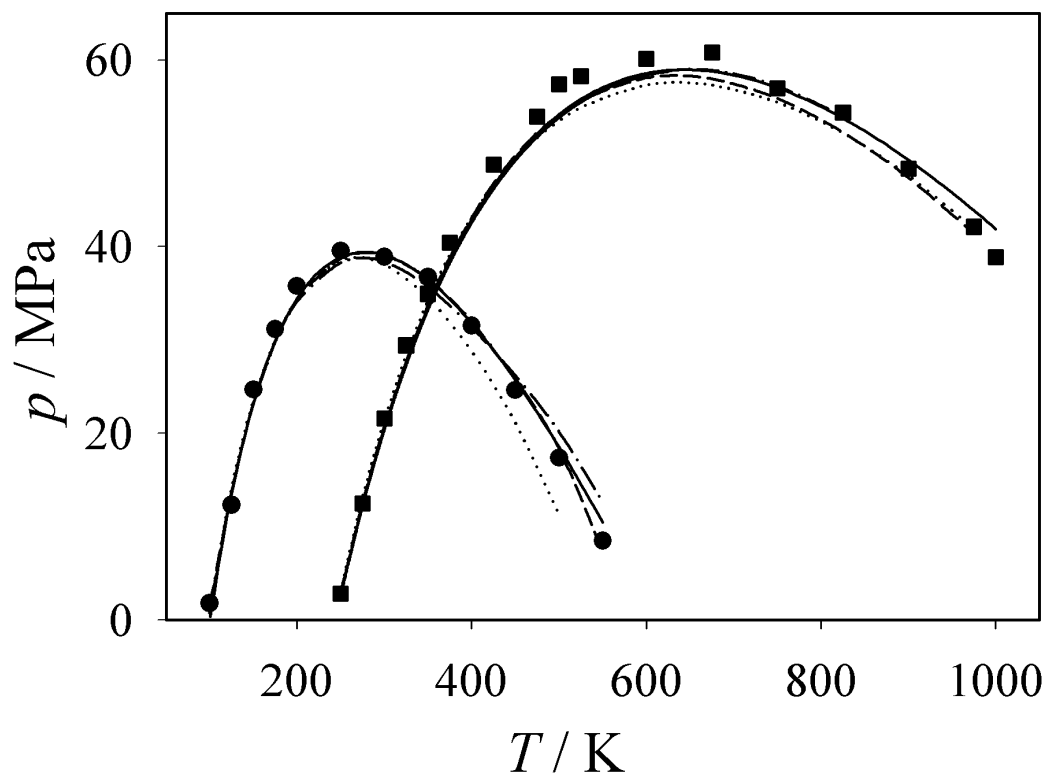


Fig. 2. Vrabc et al.

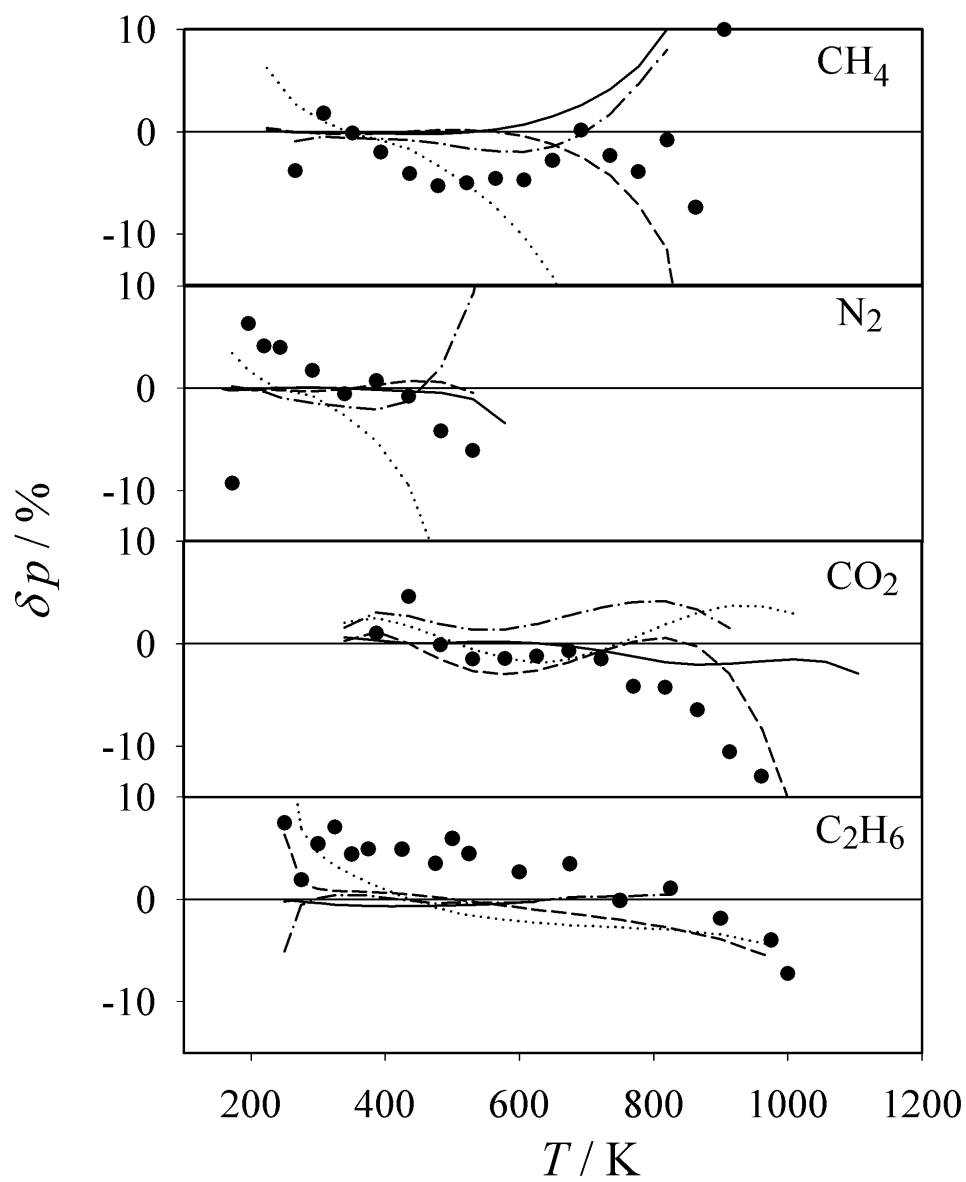


Fig. 3. Vrabec et al.

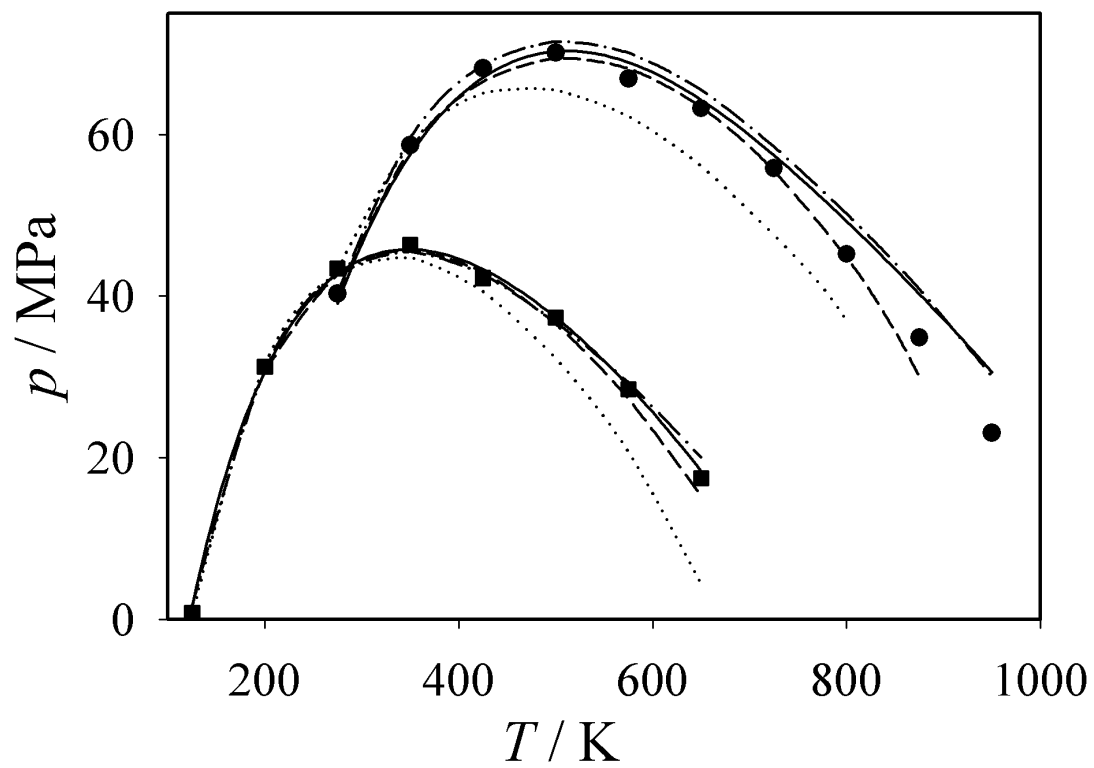


Fig. 4. Vrabc et al.

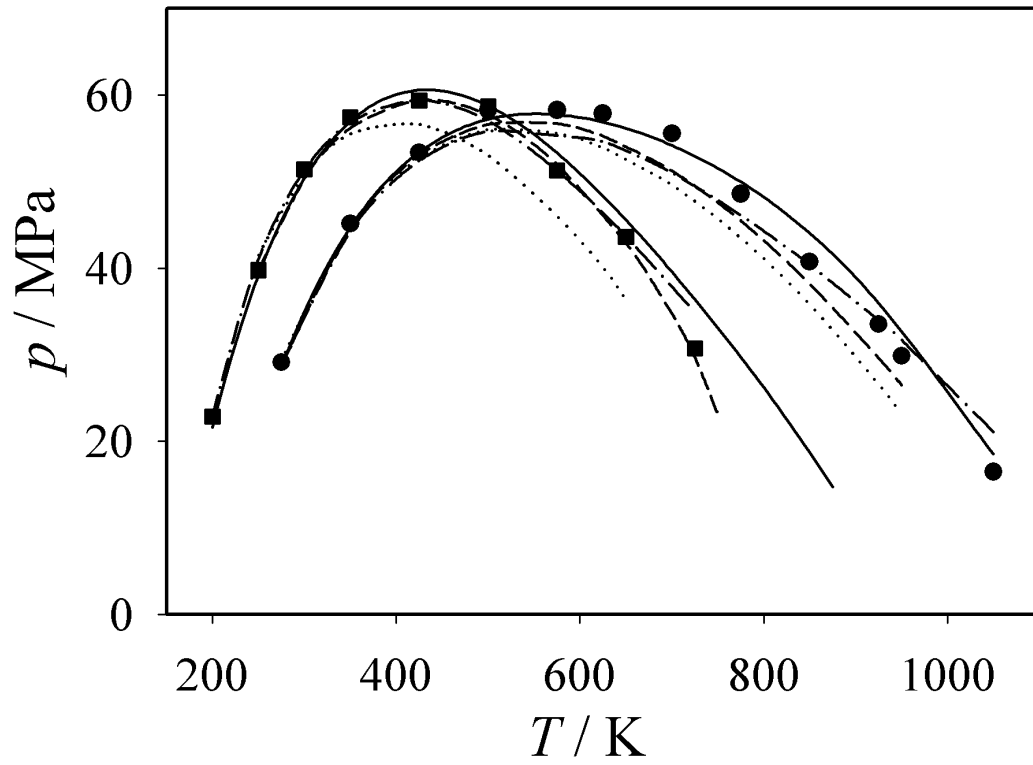


Fig. 5. Vrabc et al.

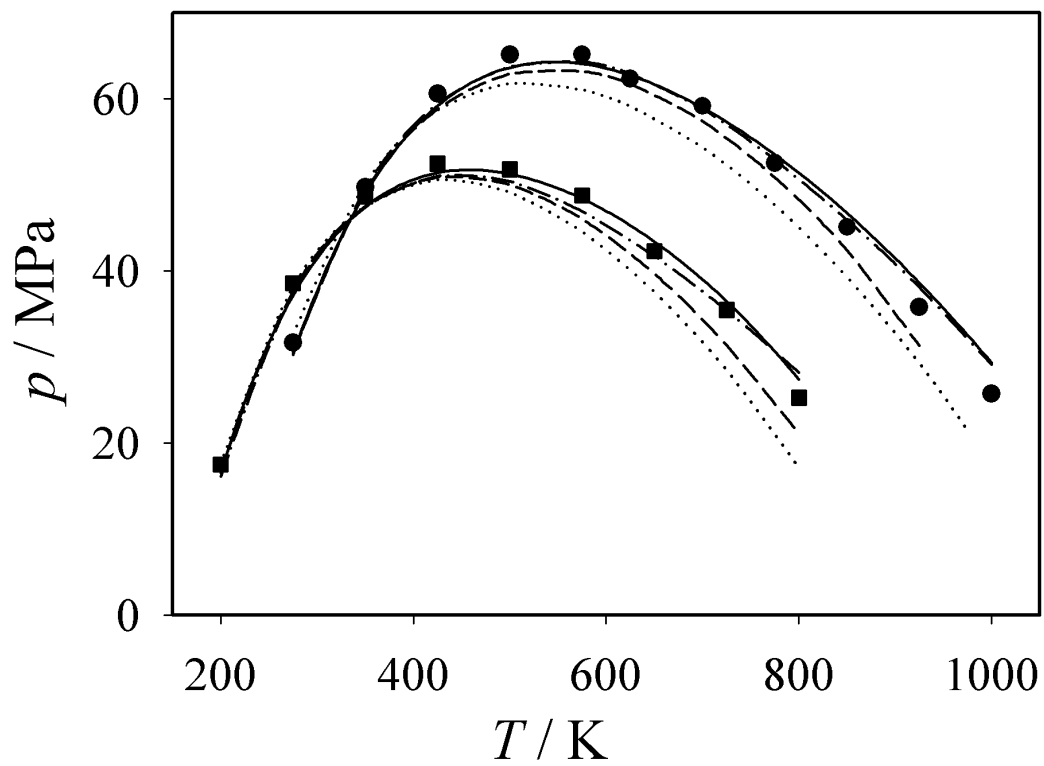


Fig. 6. Vrabc et al.



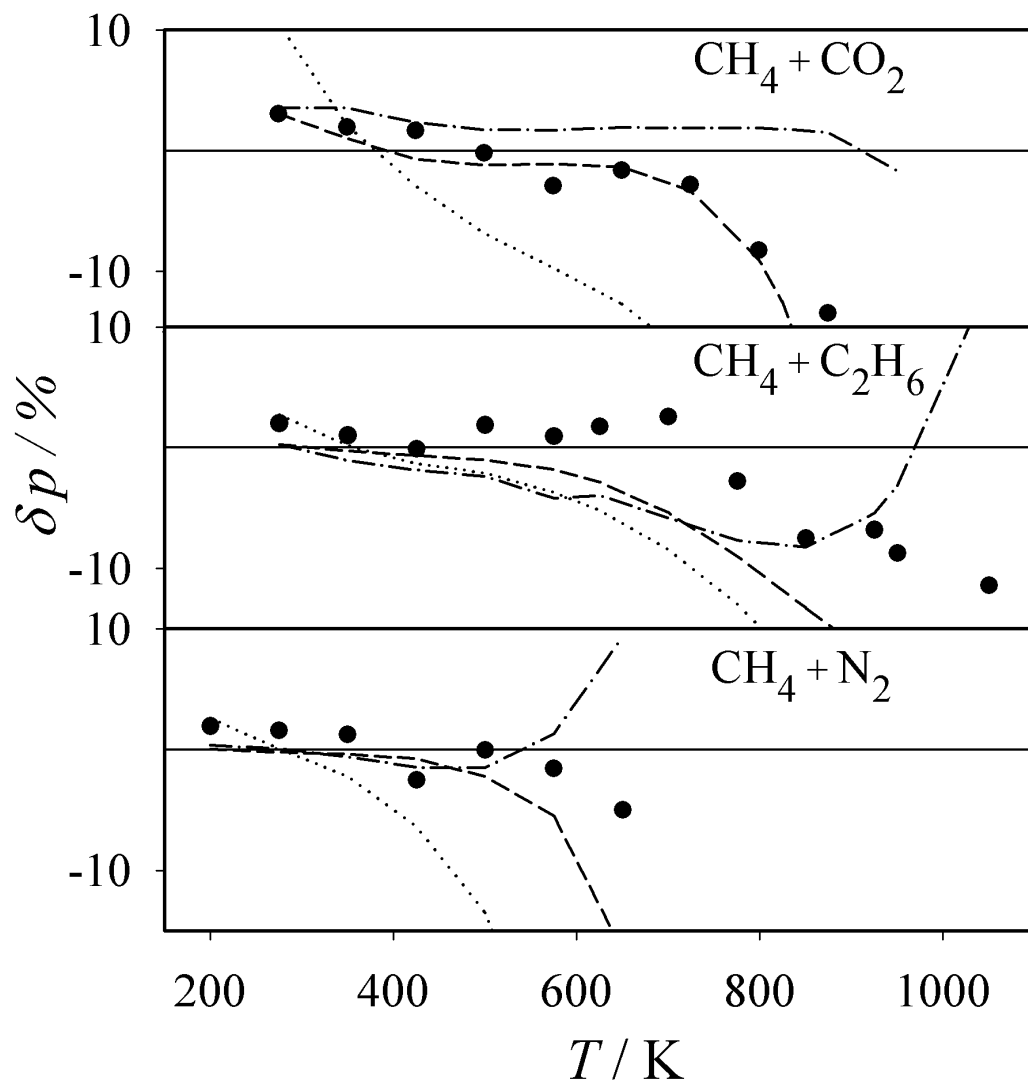


Fig. 7. Vrabec et al.

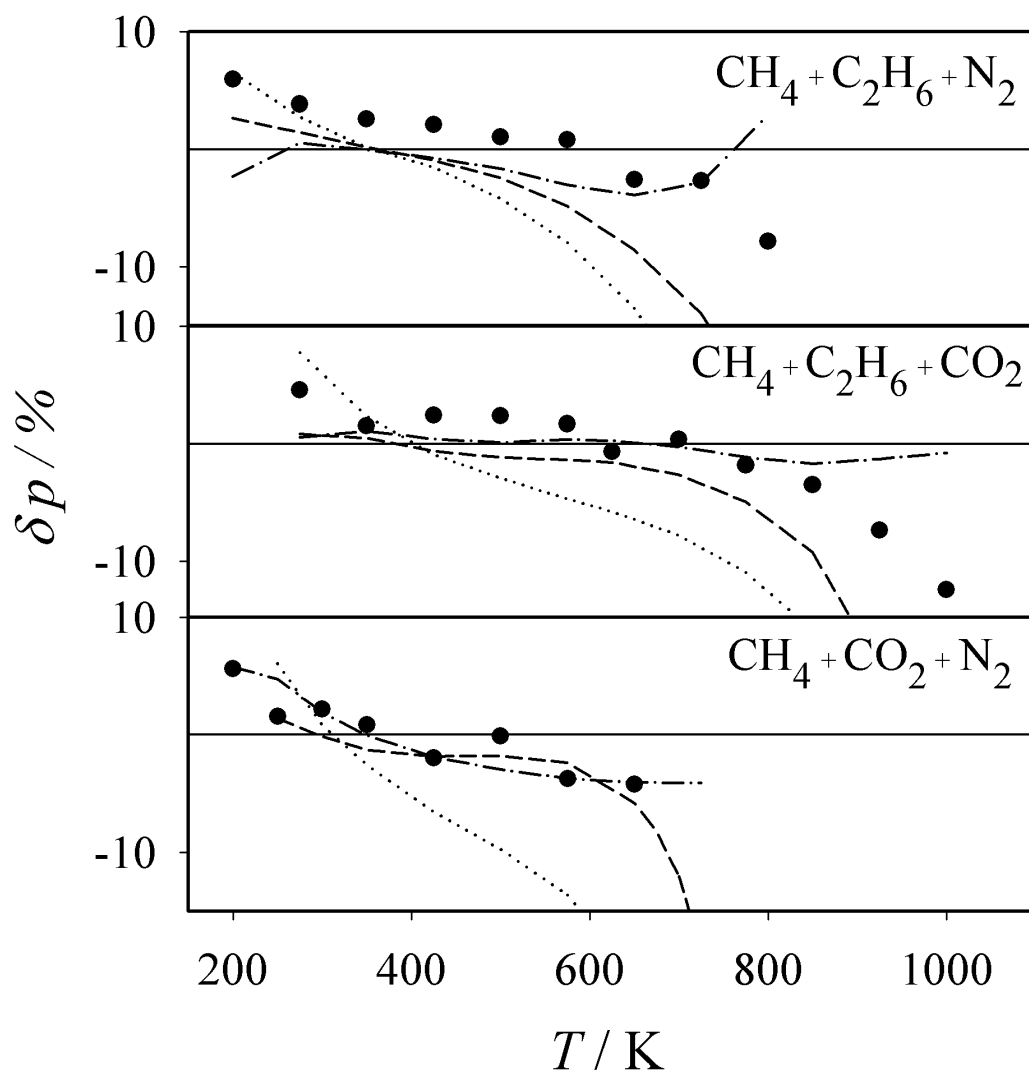


Fig. 8. Vrabec et al.